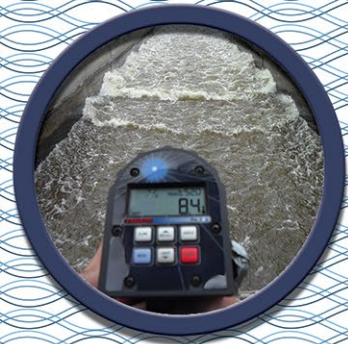# Laboratory and field testing of a handheld radar to measure the water velocity at the surface of open channels

S. Tamari

F. García

J. I. Arciniega-Ambrocio

A. Porter

Pour Natalia et Isabelle, qui aiment se baigner à "Las Estacas".

LABORATORY AND FIELD TESTING OF A HANDHELD RADAR TO MEASURE THE WATER VELOCITY AT THE SURFACE OF OPEN CHANNELS

S. Tamari

IMTA, Paseo Cuauhnáhuac 8532,
Jiutepec Mor. 62550, Mexico (tamari@tlaloc.imta.mx)

F. García

ENGEES, 1 quai Koch,
67070 Strasbourg, France

J. I. Arciniega-Ambrocio

ITCh, Av. José Francisco Ruíz Massieu 5,
Chilpancingo Gro. 39090, Mexico

A. Porter

MECOPAA, Miguel Lerdo de Tejada 118,
Col. Guadalupe Inn, México DF 01020, Mexico

December 2013

C O N T E N T

A B S T R A C T

Among the non-contact instruments to measure water velocity in open channels, two handheld radars are available on the market since ten years. Due to the lack of information about these instruments, one model was tested in the laboratory and in the field. The radar was able to estimate the velocity of a water surface within $[p = 0.95] \pm 0.3$ m/s at medium velocities (from 0.3 to 3 m/s) and within $\pm$ 10 % of the measured value at large velocities (up to at least 6 m/s). Although this is not very accurate, the ease of using handheld radars still makes them attractive to quickly estimate discharge at some gauging stations, safely determine maximum water velocity during a flood and investigate how water flows under difficult access conditions (*e.g.* very shallow channels or the straight part of some spillways).

Even though the tested radar has provided velocity data in the range of what was expected *a priori*, some biases were found. On the one hand, the radar was not working well at too low incidence angles and it was tending to underestimate the reference data, which could be due to the rather large beam width of the radar. On the other hand, the radar was tending to estimate a lower velocity when looking downstream instead of upstream. More studies are necessary to know if this is due to an inaccurate data processing algorithm of the tested instrument or if this is a general feature of microwave Doppler radars when used in open channels under clear weather conditions. Meanwhile, it is a good precaution to compare -whenever possible- the velocities obtained with a radar looking upstream and downstream.

Keywords: Surface Velocity Radar (SVR); Doppler radar; microwave; water velocity; open channels; gauging.

A C K N O W L E D G E M E N T S

Any reference to a commercial model and its manufacturer is for identification purposes only, and does not represent an endorsement of the product.

1 . I N T R O D U C T I O N

In Hydraulics, *current meters* are light instruments (< 10 kg) designed to measure the velocity of a small water volume (< 1 dm³). They are useful in open channels (artificial channels and rivers) to determine the discharge or investigate some certain hydrodynamic features. The most common instruments for field applications are [ISO 2007, Rantz & Col. 1982, Turnipseed & Sauer 2010]: mechanical current meters (MCM), electromagnetic velocimeters (EMV) and acoustic Doppler velocimeters (ADV). Acoustic Doppler current profilers (ADCP) mounted on a floating platform can be used as well [*e.g.* Costa *et al.* 2006, Szupiany *et al.* 2007].

When used properly, current meters can accurately determine water velocity: their uncertainty $[p = 0.95]$ is better than ± 0.01 m/s for low velocities (below ≈ 0.5 m/s) and ± 2 % of the measured value for medium velocities (up to ≈ 3 m/s) [*e.g.* Hubbard *et al.* 2001, ISO 2007]. Nonetheless, they must be inserted into water, which is not always practical under field conditions, since it can be time-consuming (because the operator must get close to the water surface and then control the immersion depth of the meter), dangerous (especially in case of fast flow, floating debris or crocodiles), unhealthy (when a meter has to be immersed into waste water) and costly (a meter repeatedly immersed into water can get damaged due to corrosion, incrustation, clogging or fouling).

There is therefore an interest in developing instruments that can measure water velocity in open channels with no need to submerge them. Such an interest is not new: forty years ago, an optical current meter (OCM) was developed to measure velocity at the surface of open channels [Rantz & Col. 1982], but this stroboscopic device with a telescope is no longer popular. Now, other non-contact techniques for open channels are emerging. For field applications, the two main techniques are image velocimetry (LSPIV/STIV) [*e.g.* Fujita *et al.* 2007, Le Coz *et al.* 2010] and Doppler radar (considered in this study). Unfortunately, none of these is still operational to determine velocity below the water surface (*i.e.* at a depth > 0.2 m). In this case, it is worth noting that measuring the water velocity only at the free surface -instead of measuring it at different depths- is still considered a reliable -although less accurate- method to estimate discharge in open channels [Rantz *& Col.* 1982, ISO 2007]; several researchers are currently testing [*e.g.* Costa *et al.* 2006, Lee & Julien 2006, Dramais *et al.* 2013] and trying to improve [*e.g.* Le Coz *et al.* 2010, Negrel *et al.* 2011] this method.

Among the non-contact instruments to determine velocity in open channels under field conditions, two handheld radars are available on the market since ten years. Although they look attractive for their rather low cost (< 4,500 USD) and ease of use (**Fig. 1**), little is known about their performances. The goal of this study was therefore to test a handheld radar to determine the velocity at the surface of open channels.
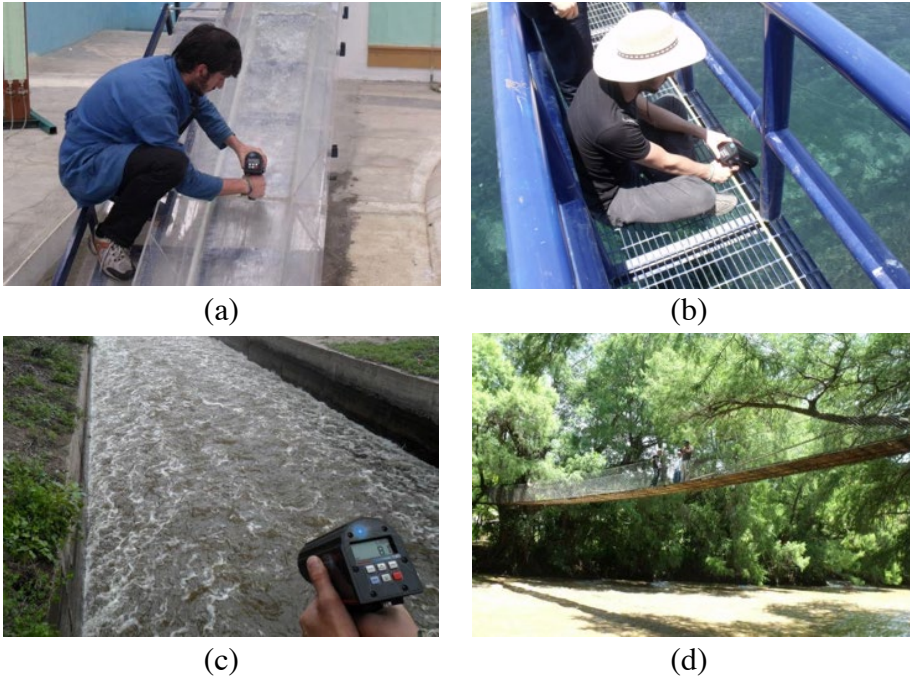
Fig. 1. Different types of sites where the handheld radar was tested:

(a) plane part of a laboratory spillway (case "L.9" of **Table 1**),
(b) irrigation channel (case "F.1"),
(c) rapid with rolling waves (case "F.4") and
(d) river with breaking waves (case "F.5").

2.1. What is known about the handheld radars ?

A *radar* is a remote sensing system that sends an electromagnetic signal of a given frequency to a target and then measures some properties of the signal that is sent back (time delay, Doppler shift and/or intensity) in order to determine its distance, speed and/or texture. [1] There are radars of different signal frequencies and designs, depending on their purpose and level of sophistication [*e.g.* Ulaby *et al.* 1981]. In particular, the *Doppler radars* are designed to determine the speed of a target.

Handheld radars look like a pistol (for this reason, they are often called *radar gun*). They can be defined as *monostatic* (the receiving antenna is near the emitting antenna) and *microwave* (they emit a signal in the microwave range) Doppler radar, designed to be easily transported by a walking person and operated from a steady position. The current instruments of this type are *Continuous Wave* (a low cost technology that does not allow the instrument to measure the distance to a target) and *K-band* (operating frequency between 18 and 27 GHz) or *Ka-band* (operating frequency between 27 and 40 GHz) radar.

---

1   The purpose of the first radars was to determine the distance to a target. For this reason, the word "radar" is an acronym for *RAdio Detection And Ranging*. Nonetheless, the word "radar" is now used in a more general sense.

Handheld radars were originally developed to determine the speed of cars [*e.g.* Jendzurski & Paulter 2008]. They have also become popular to determine the speed of animals and sporting balls [*e.g.* Newton & McEvoy 1994]. The idea of using similar instruments to determine water velocity in open channels was patented ten years ago [Smith *et al.* 2003]. However, determining the velocity of a water surface is not the same as determining the speed of a single solid object, in terms of data acquisition and processing. This emphasizes the need to test handheld radars designed to measure water velocity. There are currently two models of this type (called *surface velocity radar* by their manufacturers). Both look very similar for their shape and specifications; it is worth noting that their *(3 dB) beam width* is large in practice (12°) and that they emit a signal with a *circular polarization* (whereas the other radars for studying water usually use linear polarization: HH and/or VV). Although some authors seem to use handheld radars routinely to estimate discharge in rivers [*e.g.* Corato *et al.* 2011], little has been published about their performances:

- First, the "SVR" model from Decatur Electronics [2011] has an operating frequency of 24 GHz (*K-band*). Its claimed uncertainty [$p = 0.95$] [2] is ± 10 % of the measurement for a range from 0.3 to 9 m/s. A few evaluations of this instrument [Song *et al.* 2006, Fulton & Ostrowski 2008, Zolezzi *et al.* 2011, Dramais *et al.* 2011, 2013] suggest that it can indeed estimate surface velocity within ± 10 % for medium to large velocities ($\approx$ 0.5 - 5 m/s), but does not always operate at low velocities (< 0.5 m/s).

- Second, the "Stalker Pro II SVR" model from Stalker Radar [2008] has an operating frequency of 35 GHz (*Ka-band*). Its claimed uncertainty [$p = 0.95$] is ± 0.2 m/s for a range from 0.2 to 18 m/s. Compared to the previous radar model, its maximum operating velocity is therefore claimed to be larger (twice) and it is claimed to be more accurate at large velocities (> 2 m/s). In addition, it can measure incidence angles smaller than 40° (which can be useful for studying steep channels). Until now, there is no publication about the performances of the "Stalker Pro II SVR" radar; this model will be considered below.

---

2   In the following, *any uncertainty that is reported by a manufacturer without specifying its confidence interval is assumed to be a standard uncertainty* [$p = 0.68$]. In this case, we report a twice larger uncertainty, considering a 95 % level of confidence [$p = 0.95$].

Due to the lack of information about the performances of handheld radars in the field of Hydraulics, some concepts about the Doppler radar are reviewed in the next section, in order to better know what can be expected from these instruments.

2.2. PRINCIPLE OF OPERATION OF A HANDHELD RADAR

As for any other fixed and monostatic Doppler radar, a handheld radar determines the velocity of a target by sending a signal of a given frequency (f_0, Hz) to the target, retrieving the backscattered signal and determining its frequency (f, Hz). The *Doppler effect* is used by the instrument to internally compute the *radial velocity* of the target, that is, the component of its velocity relative to the radar's line-of-sight (V_r, m/s):

$$V_r = -\frac{c_a}{2}\frac{\Delta f}{f_0} \tag{1}$$

where c_a is the speed of light through the air ($\approx 3 \times 10^8$ m/s) and $\Delta f = f_0 - f$ is the *Doppler shift* (negative when the target gets closer and positive when it goes away). So, unless the radar is placed exactly in front of a moving target, a trigonometric correction must be applied to estimate the velocity of the target in its main direction of movement.

Consider a radar oriented in such a way (*e.g.* from a bridge) so that it looks in the main direction of a stream (**Fig. 2**). Provided that the radar signal is backscattered (as discussed in Section 2.4) and assuming that it is emitted as a narrow beam (as discussed in Section 4.2), the velocity of the water surface (V_s, m/s) can be estimated as:

$$V_s = \frac{V_r}{\sin\theta} \tag{2}$$

where V_r (m/s) is the radial velocity of the water surface and θ (°) is the radar's incidence-angle relative to the water surface.

At the scale of several metres, it can be usually assumed that the water surface of open channels is a horizontal plane: this is realistic (with a tolerance of ± 1°) provided that the channel slope is gentle (< 0.017 m/m) and that there is no hydraulic jump. In this case, the angle θ of **Eq. 2** is simply the *incidence angle* of the radar (θ_o), *i.e.* the angle between its line-of-sight and the vertical. Commercial handheld Doppler radars have a built-in inclinometer, so that they can automatically determine such an angle and use it to estimate the velocity of a horizontal water surface [Smith *et al.* 2003].

Next, the case of a plane but inclined water surface will be also considered. This situation occurs in steep artificial channels and in the middle part of some spillways. In this case, the angle of **Eq. 2** is: $\theta = \theta_o - \beta$ for a radar looking upstream, and $\theta = \theta_o + \beta$ for a radar looking downstream, where β is the slope of the water surface ($0 \le \beta < 90°$). In practice, the water surface is often almost parallel to the channel bottom and edges, which can be easily checked visually. If so, the angle β can be rapidly estimated by measuring the channel's slope with the built-in inclinometer of a handheld radar or any other inclinometer. Nevertheless, it becomes more difficult to determine the angle β when the water surface is curved (as it occurs over many spillways); such a situation is out of the scope of this study.
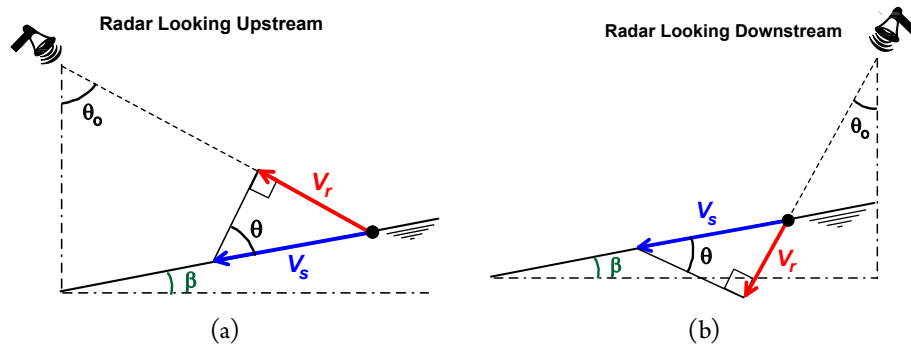
Fig. 2. Geometrical framework considered to determine the velocity of a free water surface using the radar (symbols are explained in Section 2.2): the instrument is placed above water and is looking (a) upstream or (b) downstream.
The water surface is assumed to be a plane, that can be inclined ($0 \le \beta < 90°$).

2.3. WHICH INCIDENCE ANGLE FOR THE RADAR ?

To reduce the effect of the trigonometric correction (**Eq. 2**) as much as possible, a radar should be placed so that it looks at the water surface with a relative incidence angle as large as possible ($\theta \rightarrow 90°$, so that $\sin\theta \rightarrow 1$). Nonetheless, when a handheld radar looking at a water surface is oriented with a too large incidence angle, it becomes difficult in practice to know at what it is pointing. During this study, no attempt was made to use the handheld radar with a relative incidence angle larger than 70°.

Assuming that V_r and θ are normally-distributed and independent random variables [JCGM 2008], a simple model to estimate the uncertainty of V_s can be derived from **Eq. 2**; this model is slightly more rigorous than the one proposed by Fulton & Ostrowski [2008]:

$$U(V_s) \quad = \quad \sqrt{\left(\frac{1}{\sin\theta}\right)^2 U^2(V_r) \;+\; \left(\frac{V_s}{\tan\theta}\right)^2 U^2(\theta)} \tag{3}$$

where $U(\bullet)$ denotes the uncertainty of each variable (at a given confidence level); please note that the term $U(\theta)$ must be expressed in radians. Strictly speaking, the model does not agree with what is claimed by the manufacturers of handheld radars (Section 2.1); in fact, it predicts that the uncertainty of the surface velocity $U(V_s)$ is neither a constant value nor a fixed proportion of the measured value.

In the case of the studied radar, assuming that its claimed uncertainty is for the radial velocity: $U(V_r) = 0.2$ m/s [$p = 0.95$] and considering that the claimed uncertainty of its built-in inclinometer is: $U(\theta) = 0.07$ rad (4°) [$p = 0.95$] [Stalker Radar 2008], the expected uncertainty $U(V_s)$ can be computed using **Eq. 3** for different scenarios (different values of V_s and θ). The results (**Fig. 3**) suggest that the radar should be oriented with an incidence angle $\theta > 45°$, otherwise its uncertainty will rapidly increase.
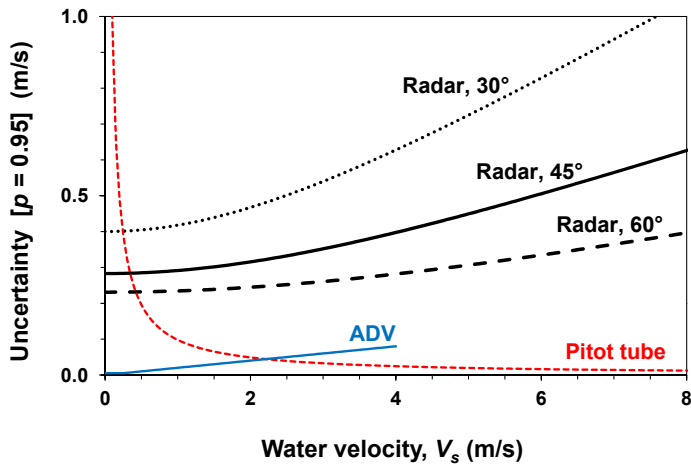
Fig. 3. Expected uncertainty of the tested radar (see Section 2.3) as a function of water velocity (V_s) for three incidence angles (θ = 30, 45 and 60°). The expected uncertainty of two current meters used as a reference is also shown: an ADV and a Pitot tube (see Section 3.3).

2.4. DETECTION OF A WATER SURFACE BY A MICROWAVE RADAR

To be able to determine the velocity of a water surface, a Doppler radar must first detect it: the signal sent by the instrument must be reflected by the water in such a way that it goes back to the instrument and can be processed. This phenomenon has been studied for 50 years in the laboratory and on the sea (for more details, see Section A.1). Considering that the handheld radar emits microwaves, the backscattering of its signal by water (at least, for intermediate incidence angles: $20 \leq \theta \leq 70°$) is currently described by the *Bragg / composite surface* theory [*e.g.* Hasselmann *et al.* 1985, Plant & Keller 1990, Plant *et al.* 2004].

On the one hand, the theory considers that the microwaves are mostly backscattered by small water waves (traveling nearly in the plane of incidence, either toward the radar, either away from it), *i.e. ripples* with a wavelength $\Lambda_B \approx 6$ mm in the case of the studied radar (for more details, see Section A.2). In open channels, these ripples can be produced by external factors (the wind and the rain) and internal factors (the distortion of larger waves and the turbulence of water). On the other hand, the theory considers that the ripples backscattering the radar signal are mostly driven by larger water waves (for more details, see Section A.3). In open channels, these larger waves (gravity-capillary waves and hydraulic boils) are due to the wind and turbulence of water. On average, they are assumed to move at the velocity of the water surface.

The above theory predicts that the tested radar will not work if there are virtually no ripples on a water surface, as it may occur under low water flow and clear weather conditions [*e.g.* Plant *et al.* 2005] or if there is an oil film on the water [*e.g.* Gade *et al.* 1998]. It also predicts that the raw data recorded by a radar (a time-series of Doppler shifts) are "noisy". The main reason for that is that each water wave (ripples and larger waves) tends to propagate in several directions. So, a radar should detect water waves that sometimes move faster than the average water surface ("advancing waves") and that sometimes move slower ("receding waves").

Ideally, the histogram of the raw data recorded by the radar (converted into surface velocities, according to **Eqs. 1-2**) should have two peaks: one corresponding to $V_s + c_B$ and the other corresponding to $V_s - c_B$, where c_B is the *phase speed* of the water waves that backscatter the radar signal. If so, processing the raw radar data simply consists in extracting the midway point between the two peaks. However, it is often difficult to discern this theoretical couple of peaks with a microwave radar (for more details, see Section A.3). In this case, processing the raw radar data is not straightforward anymore. If data are not processed carefully, the estimated surface velocity (V_s) can be erroneous up to $\pm c_B$ [Plant *et al.* 2005]. For the studied radar, $c_B \approx 0.3$ m/s (Section B.1); it is worth noting that the minimum expected uncertainty of the radar (computed from **Eq. 3** with $\theta = 45°$) is close to this value (**Fig. 3**).

2.5. Difficulty in interpreting the velocity measured by a radar

Assuming that the data have been averaged over a sufficiently long period of time, the surface velocity determined by a Doppler radar (V_s) can be decomposed as an algebraic sum of four terms (**Fig. 4**):

$$V_s \quad = \quad V \quad + \quad W \quad + \quad U_s \quad + \quad \upsilon \tag{4}$$

where V is the drift caused by the underlying current (m/s), W is the drift caused by the wind blowing in the direction of the radar's line-of-sight, U_s is the Stokes drift (m/s) and υ is an eventual bias due to the way a radar "sees" a water surface (m/s). Considering the goal in Hydraulics is to determine the underlying current (V), taking it to be equal to the surface velocity measured by a radar (V_s) may lead to three types of systematic errors:

- *Wind effect (W)* - In practice, the drift of a water surface caused by the wind can be roughly estimated as [*e.g.* Plant *et al.* 2005]: $W \approx 0.02 \times W_{10}$, where W_{10} (m/s) is wind speed measured at 10 m above the surface. During this study, the handheld radar was tested under low wind conditions, at most equivalent to a *gentle breeze* on the Beaufort scale ($W_{10} < 5.5$ m/s); the wind effect was therefore expected to be rather small ($W < 0.1$ m/s).

- *Stokes drift (U_s)* - The Stokes drift is accounted for by a Doppler radar (as well as by small surface drifters), but not by a conventional current meter that would be maintained at a fixed position and just below the water surface [*e.g.* Monismith & Fong 2004]. So, this could be a cause of systematic difference between the radar and a conventional estimation of water velocity. Nevertheless, the Stokes drift was expected to be rather small for most of the studied channels: $U_s \leq 0.14$ m/s, at least in the laboratory (see Section B.2).

- *Bias term due to the radar (υ)* - Due to the specific motion of the water waves that backscatter the radar signal, there may be a systematic difference ($\upsilon \neq 0$) between the surface velocity determined by a Doppler radar and the true surface velocity for a number of reasons; this will be discussed further below (Section 4).

Microwave radar

Wind W

**Larger waves
and vortices**

**Stokes
drift** U_S

Ripples

**Underlying
current** V
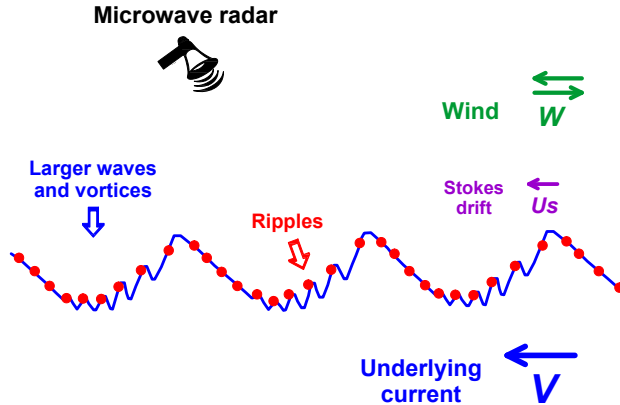
Fig. 4. Diagram showing which details of a water surface should be "seen" by the tested radar.

Most of the radar signal is expected to be backscattered by some parts (points on the diagram) of small water waves (ripples), which should be driven by larger waves.

Although the water waves tend to move in several directions at their own phase speed, on the average they are assumed to be advected by the underlying current (the drift caused by the wind was expected to be small for the studied channels); in this case, the Stokes drift should be in the direction of the current.

2.6. Experience with microwave radars in open channels

As shown, it is not so simple to use a radar to estimate the velocity of a water surface. In this context, microwave radars with different configurations have been tested over open channels over the last fifteen years.

Above all, prototypes [Contreras & Plant 2004, Costa *et al.* 2006, Plant *et al.* 2005, Fulton & Ostrowski 2008] and commercial instruments [Song *et al.* 2006, Dramais *et al.* 2011, 2013, Sung-Kee *et al.* 2012] fixed to a bridge (radar looking in the direction of the main stream) have been tested Prototypes [Costa *et al.* 2006, Plant *et al.* 2005] and commercial instruments [Sung-Kee *et al.* 2012] located at a channel bank have been also tested. Prototypes moved across a channel using a cableway [Costa *et al.* 2006, Plant *et al.* 2005] or a helicopter [Plant *et al.* 2005] have been tested as well. It is worth noting that a radar with an operating frequency of 10 GHz (*X-band*) and a design very similar to that of the commercial handheld radars has been described and tested by Lee & Julien [2006]; nonetheless, it seems to have been forgotten for an unknown reason.

All the mentioned field testing suggest that microwave radar can usually determine the surface velocity of open channels with an uncertainty [$p = 0.95$] of ± 0.2 m/s, which is consistent with that claimed by the manufacturers of handheld radars. Nevertheless, testing have been conducted in rivers but not in artificial channels (where the roughness of the water surface may be different due to different turbulence conditions) and only for water velocities ≤ 5 m/s.

| 3 . M A T E R I A L S |
| A N D   M E T H O D S |

3.1. SITES WHERE THE RADAR WAS TESTED

Based on the literature review (Section 2), it was decided to test the handheld radar over a series of open channels (**Table 1**):

- *Wide range of water velocities* - The radar was tested for the widest range of velocities as possible, *i.e.* from 0.3 up to at least 6 m/s. To achieve this range, tests were performed not only over horizontal channels, but also over the plane part of inclined channels (slope as large as 28°). It was not sure whether the radar would work under clear weather conditions at low velocities (< 0.5 m/s), and the comparison with conventional current meters was quite challenging at large velocities (> 3 m/s).

- *Several types of open channels and flow conditions* - Compared to other radars designed to study open channels, the handheld radar can be very easily transported from one site to another, which makes it possible to rapidly test this instrument under several flow conditions. For this study, 18 sites were chosen for testing, with a special interest in artificial channels. The testing was performed in straight portions of wide (*aspect ratio* $\nu > 5$) and narrow ($\nu < 5$) channels, with different wall roughness (walls made of glass, acrylic, cement, concrete or earth and stones). Both subcritical (*Froude number Fr* < 1) and supercritical (*Fr* > 1) flow conditions were considered.

- *Clear weather conditions* - The radar was tested in the laboratory (13 sites) and in the field (5 sites). In the field, testing was made under low wind (not more than a gentle breeze) and no rain conditions. Although these conditions are convenient for the user and should ensure that the water surface is mostly driven by the underlying current, they are known to be challenging for the radar when water flows slowly. The water surface may indeed be too smooth to produce a significant backscattering of the radar signal [*e.g.* Plant *et al.* 2005].

- *No oil at the water surface* - The radar was tested over channels with clear (laboratory channels and case "F.1" in **Table 1**), turbid (cases "F.3" and "F.4") and very turbid (cases "F.2" and "F5") water, but *not* in channels contaminated by gasoline or detergent (where the presence of an oil film could prevent the radar from detecting the water surface) [*e.g.* Gade *et al.* 1998].

Table 1. Sites where the handheld radar has been tested.

Code	Location	Name	Channel type	Shape	Channel walls	Length of the straight part (m)	Channel slope (β, °)	Bottom width (b, m)	Surface width (b_s, m)	Water level (h, m)	Aspect ratio (ν = b/h)	Surface velocity (V_s m/s) (a)	Froude number (Fr) (b)	Reference techniques (c)	No. of data
L.1	IMTA Laboratory	*Canal Largo*	Horizontal	Rectangular	Glass	50	0.0	1.0	1.0	0.15 - 0.30	3 - 7	0.4 - 1.2	0.2 - 0.4	ADV, EMV, Pitot	7
L.2	"	*Outlet of Coyotes*	"	"	Cement	10	0.0	1.0	1.0	≈0.40	≈ 2	0.4	≈ 0.2	EMV	1
L.3	"	*Outlet of Hervidero*	"	"	"	8	0.0	0.8	0.8	0.28	3	0.25	0.2	ADV, Pitot, EMV	1
L.4	"	*Outlet of Naranjos*	"	Trapezoidal	Acrylic	1	0.0	0.7	0.8	0.03	26	2.7	3.6	ADV, Pitot, EMV	1
L.5	"	*Inlet of Vista Hermosa*	"	"	"	2	1.1	0.3	0.4	0.25	1	1.2	0.7	EMV	1
L.6	"	*Spillway of Coyotes*	Inclined	"	Cement	6	2.9	0.4	0.5	0.07 - 0.08	5 - 6	2.3 - 2.7	1.9 - 2.3	ADV, Pitot, EMV	3
L.7	"	*Spillway of Hervidero*	"	"	Acrylic	5	5.4	0.3	0.4	0.05 - 0.07	5 - 7	2.4 - 3.3	2.3 - 3.4	ADV, EMV	3
L.8	"	*Spillway of Naranjos*	"	"	"	3	7.2	0.7	0.8	0.03 - 0.04	22 - 26	2.1 - 2.7	2.7 - 3.4	ADV, Pitot, EMV	2
L.9	"	*Spillway of Vista Hermosa*	"	"	"	3	17.9	0.3	0.3	0.03 - 0.06	5 - 11	2.5 - 4.2	2.2 - 5.3	Pitot, ADV, EMV	4 (d)
L.10	"	*Canal Inclinable*	Tilting	Rectangular	Glass	18	0.2 - 1.0	0.6	0.6	0.08 - 0.24	3 - 7	1.4 - 2.1	0.6 - 2.2	ADV, Pitot	14
L.11	CFE Laboratory	*Fondo (Yesca)*	Covered	"	Acrylic	5	0.0	0.6	0.6	≈0.30	≈ 2	2.2 - 4.5	≈ 0.8 - 1.7	Pitot	9
L.12	"	*Inlet of Aeradores (Yesca)*	Horizontal	"	"	≈ 5	0.0	0.3	0.3	0.25	1	3.6	1.7	Pitot, ADV	1
L.13a	"	*Spillway MI of Aeradores (Yesca)*	Inclined	"	"	≈ 4	27.6	0.3	0.3	0.20	1.5	5.5 - 5.6	2.7 - 2.8	Pitot	3 (d)
L.13b	"	*Spillway C of Aeradores (Yesca)*	"	"	"	≈ 5	27.6	0.3	0.3	0.05 - 0.14	2 - 7	5.0 - 5.7	3.2 - 5.0	Pitot	3

Table 1. Sites where the handheld radar has been tested (Cont.).

Code	Location	Name	Channel type	Shape	Channel walls	Length of the straight part (m)	Channel slope (β, °)	Bottom width (b, m)	Surface width (b_s, m)	Water level (h, m)	Aspect ratio (ν = b/h)	Surface velocity (V_s m/s) (a)	Froude number (Fr) (b)	Reference techniques (c)	No. of data
E1	18° 43' 24.10" N 99° 6' 42.60" W	*Las Estacas* (29/12/2011)	Irrigation	Trapezoidal	Concrete	300	0.0	1.7	6.0	1.65	2	1.2	0.3	ADV, EMV	31
F.2	19° 32' 22.20" N 100° 29' 13.10" W	*Tuxpan* (07/06/2011)	"	Rectangular	"	200	0.0	6.0	6.0	0.98	6	0.9	0.2	ADV	12
F.3	18° 54' 42.21" N 98° 5' 55.35" W	*Valsequillo* (20/06/2012)	"	"	"	50	0.0	8.0	8.0	2.82	3	2.4	0.3	ADV	16
F.4	18° 40' 55.50" N 97° 43' 28.00" W	*Tepalzolco* (21/06/2012)	Rapid with rolling waves	"	"	950	2.0	5.0	5.0	≈ 0.25	≈ 20	≈ 8.7	≈ 4.0	PIV	11
F.5a	18° 35' 59.65" N 99° 22' 29.47" W	*Amacuzac* (15/08/2012)	River with breaking waves	Irregular	Earth and stones	50	0.0	≈ 38	38	1.00	40	2.5	0.6	n.a.	16
F.5b	"	*Amacuzac* (21/08/2012)	"	"	"	"	"	"	38	0.98	40	2.5	0.6	MCM	17

(a) At the central part of each channel.

(b) See **Eq. B.3**.

(c) The technique finally chosen as the reference is the first one of each list (see Section 3.3).

(d) Seven data obtained with the radar looking downstream over two steep channels (cases "L.9" and "L.13a") have been discarded, because we unfortunately realized after testing that they had been taken with a too low incidence angle of: θ ≈ 41 - 45 ° (see Section 4.2).

3.2. CONDITIONS FOR USING THE RADAR

The only parameter for configuring the tested radar was its "power output", which was set at 20 mW (as recommended by the manufacturer for taking data close to a water surface).

After that, taking a measurement with the tested radar was easy: once oriented in the main direction of a stream, its built-in inclinometer was used to incline the radar to a desired incidence angle ($\theta_o = 90° - \phi_o$, where ϕ_o is the *grazing angle* that was actually displayed by the radar); the radar was then maintained in the same position and its trigger was pressed. About 30 s later, the radar was usually displaying a symbol saying whether water was moving forward or downward and an average velocity data (V_s^m); because the radar has been designed to be used over horizontal channels, this data is a projection in an horizontal plane of the determined radial-velocity ($V_r = V_s^m \times \sin\theta_o$).

During testing, the radar was operated as follows:

- *Radar oriented in the main-stream direction* - The radar was always oriented in the main-stream direction. So, field testing was made from bridges of gauging stations. No attempt was made to use the radar from a channel edge; in this case, there was no need to correct the radar data for the azimuth angle relative to the channel direction (as done by Lee & Julien [2006]) and there was no concern with secondary or cross currents (as discussed by Plant *et al.* [2005]).

- *Radar looking upstream / downstream* - Each time, a measurement was taken with the radar looking upstream and another with the radar looking downstream. In the laboratory, special attention was paid to locate the radar so that it was pointing at the same part of a channel. While this was not possible in the field, the studied channels were long and uniform enough to reasonably assume that the transversal velocity-profile was the same along the section where the measurements were taken.

- *Radar located as close as possible to the water surface* - As a first approximation (Section A.5), the tested radar should "see" an area at the water surface (*footprint*), which is an ellipse with a transversal diameter: $D_T \approx 0.2 \times L$, where L (m) is the distance to the surface in the line-of-sight direction. It must be recognized that this relation applies only if the distance L is larger than a certain value, which is: $L_f = 0.6$ m for the studied radar (Section A.4). In the field, the radar was located at $3 \leq L \leq 10$ m, resulting in $0.6 \leq D_T \leq 2$ m. In the laboratory, it was empirically [3] located at $0.1 \leq L \leq 0.3$ m; D this is smaller than L_f, resulting in $D_T < 0.12$ m. Thus, it was felt that the area sampled by the radar was not too large (so that the radar data could be used on channels with a width $b \leq 0.3$ m and so that its data could be compared to the data provided by current meters).

- *Measurements taken rather quickly* - Once a first value for the average velocity was displayed by the radar, the instrument was left to take more data and average them during ≤ 20 - 40 s. This duration was usually sufficient to achieve repeatable data with a tolerance of ± 0.15 m/s. [4]

- *Radar's inclinometer considered as unbiased* - According to its manufacturer [Stalker Radar 2008], the radar's built-in inclinometer has an uncertainty $[p = 0.95]$ of $\pm 4°$. This was checked against a comparison with an external inclinometer with a tolerance $< 1°$ (model "MTi", Xsens Technologies, Enschede, The Netherlands). Although systematic differences were found, their magnitude was always $< 2.6°$ (**Fig. 5**).

---

3   We relied on the recommendation of a manufacturer [Decatur Electronics 2011], saying: "*The radar gun makes the best measurements, when it is as close to the water surface as possible*".

4   During laboratory and field testing, two replicates were performed with the radar most of the time: one measurement was taken before using reference techniques (Section 3.3) and the other was taken after. A mean value was computed from the result of these two measurements.

- *Radar always oriented with its handle downward* - At the beginning of the study, some preliminary tests were performed to see how the handheld radar responds to different orientations: First, it was found that the instrument provides unreliable incidence angles if its handle is not in a vertical plane (roll angle ≠ 0); an interpretation would be that the radar's inclinometer measures the pitch only, but not the roll. Second, it was found that the tested radar must be oriented with its handle downward: for unknown reasons, the instrument provides unreliable velocity data if its handle is upward.

- *Intermediate incidence angle* - The radar was oriented with a relative incidence angle (θ) between 45 and 60° during normal operation. This will be discussed more in detail further below (Section 4.2).
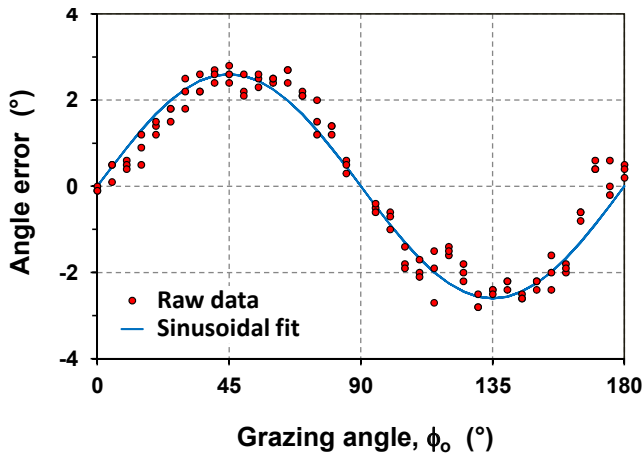

Fig. 5. Laboratory verification of the radar's built-in inclinometer.
The error is the difference between the angle displayed by the radar and the actual angle.

Please, note that the radar displays the *grazing angle* (ϕ_o),
i.e. the angle between its line-of-sight and the horizontal.

3.3. Reference techniques for testing the radar

The handheld radar was compared with five other techniques of velocimetry (**Table 2**):

- *Reference techniques in the laboratory* - In the laboratory, three types of current meters were considered as a reference: an EMV (model "Flo-Mate", Marsh-McBirney), an ADV (model "FlowTracker", Sontek/YSI) and a Pitot tube (model "630", Lambrecht). To estimate the surface velocity in open channels, these meters were located as close as possible to the water surface (sensor top at ≈ 2 cm below the surface), with special care to avoid cavitation around them during the measurements (if cavitation was observed, the meter was taken out and immersed again; if cavitation persisted, the meter's data were discarded).

  If working properly, the EMV and the ADV were expected to be several times more accurate than the studied radar at low to medium water velocities, whereas the Pitot tube was expected to be much more accurate at large velocities (**Fig. 3**). However, an inter-comparison performed at medium velocities showed that the EMV data were often in disagreement with the ADV and the Pitot tube data (**Fig. 6**); since this was occurring when the water level was low (< 8 cm), it was concluded that the EMV is not suitable for studying very shallow open channels (which could be due to the fact that its sensing part is three times higher than that of both the ADV and the Pitot tube). Therefore, most of the laboratory testing was conducted taking the ADV as the reference at low to medium velocities (< 2.5 m/s) and the Pitot tube as the reference at large velocities.

- *Reference techniques in the field* - The above mentioned ADV ("FlowTracker") was used in the field as the reference wherever it was possible to immerse it using a wading rod: low to medium water velocity (< 2.5 m/s) and water surface close to the bottom of a bridge (< 3 m). When the velocity was not too large but the water surface was too low (case "F.5" of **Table 1**), an MCM connected to a cable with a sounding weight was used as the reference. And when water was flowing very rapidly (case "F.4"), a simple PIV technique was used (Appendix C.2).

Table 2. Techniques used as a reference for estimating the velocity at the surface of open channels.

Type of meter	Model (manufacturer)	Conditions for use	Maximum velocity (m/s)	Height of the sensing part (m)	Depth at which the top of the sensing part was immersed (m)	Measuring duration (s)	Expected uncertainty (m/s) [p = 0.95]
EMV (electromagnetic velocimeter)	"Flo-Mate" (Marsh-McBirney, Frederick, Maryland)	The sensing part must be oriented in front of the main stream	6 (claimed)	0.03	≈ 0.02	40	Claimed by the manufacturer: $U(V) = 0.034 + 0.04 \times V$ (m/s)
ADV (acoustic Doppler velocimeter)	"FlowTracker" (a) (Sontek/YSI, San Diego, California)	The sensing part must be placed at ≈ 0.12 m at one side from where the velocity is measured	4 (claimed)	0.01	"	60	Claimed by the manufacturer: $U(V) = 0.005$ (m/s), if $V \leq 0.5$ m/s; $U(V) = 0.02 \times V$ (m/s), if $V \geq 0.5$ m/s
Pitot tube (connected to water manometers)	"Model 630" (Lambrecht, Goettingen, Germany)	Velocity computed from: **Eq. C.1**	No theoretical limit	"	"	≈ 240	Theoretical: **Eq. C.2** with $U(\Delta h) = 0.01$ m
MCM (mechanical current meter)	"Price AA" (b) (Rossbach, Mexico)	Meter connected to a cable with a sounding weight of 7 kg	≈ 3.5 (nominal)	0.10	≈ 0.20	60	Nominal: $U(V) = 0.01$ (m/s), if $V \leq 0.5$ m/s; $U(V) = 0.02 \times V$ (m/s), if $V \geq 0.5$ m/s
PIV (particle image velocimetry)	"Handycam" HDR-CX110" (Sony, Mexico)	Velocity computed from: **Eq. C.3**	No theoretical limit	*n.a.*	Water surface is filmed	≈ 300 (filmation)	Theoretical: **Eq. C.4**

(a) Firmware vers. 2.5

(b) Meter rated at IMTA
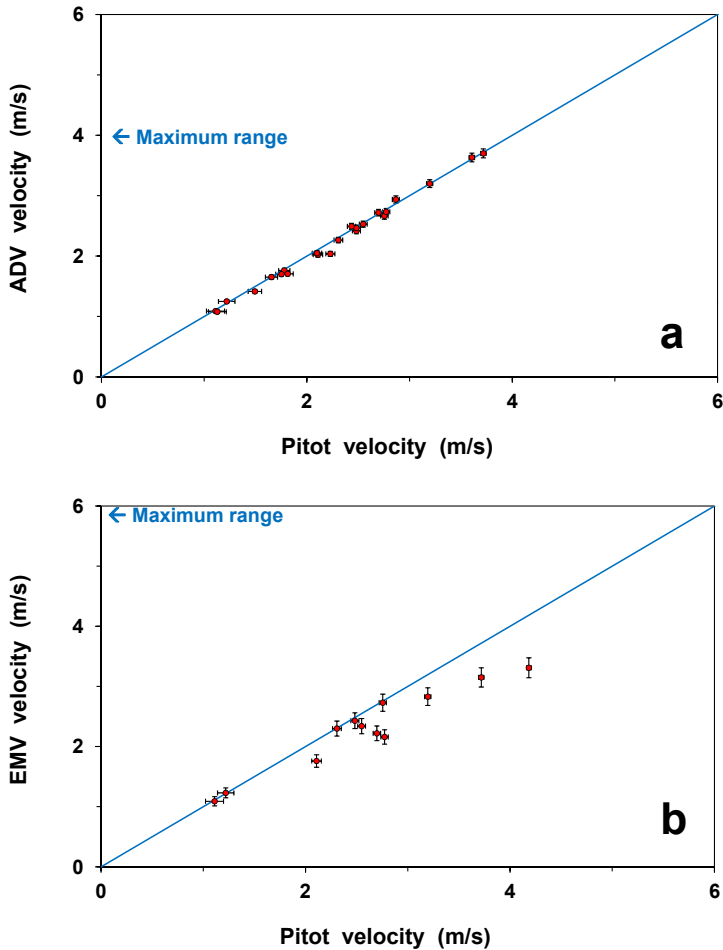
Fig. 6. Laboratory inter-comparison of three conventional current meters used during this study: (a) ADV ("FlowTracker") vs. Pitot tube; (b) EMV ("Flo-Mate") vs. Pitot tube.

Bars show the expected uncertainty $[p = 0.95]$ of each meter (see **Table 2**).
Please note that the meters were intended to be used to estimate the velocity of a water surface, therefore the top of their sensing part was located ≈ 2 cm below the surface.

<div style="border:1px solid black;">

4. RESULTS AND DISCUSSION

</div>

4.1. GLOBAL PERFORMANCES OF THE RADAR

In this section, the global results obtained with the handheld radar during normal operation (*i.e.* with a relative incidence angle between 45 and 60°) are shown. When tested in the laboratory and looking upstream, the handheld radar was found (**Fig. 7a**) to estimate water velocity at the surface of open channels from 0.3 to at least 6 m/s with an uncertainty slightly better $[p > 0.95]$ than what was expected at the beginning of this study (Section 2.3). [5] Roughly, it corresponds to: $U(V_s) \approx 0.3$ m/s at medium velocities (from 0.3 to 3 m/s) and $U(V_s) \approx 0.1 \times V_s$ at large velocities. Such an uncertainty is similar to that previously reported for the other commercial model of handheld radar (Section 2.1) and slightly larger than that previously reported for other types of microwave Doppler radars that have been tested in rivers (Section 2.6). Nevertheless, it is worth noting that the handheld radar was tested over a large set of water velocities (including > 5 m/s) and channel types (including inclined channels). [6]

More in details, it must be recognized from a regression analysis that the radar data were significantly lower than the reference data (this will be discussed in Section 4.3).

---

[5] Please note that the uncertainty of the reference techniques has been neglected because it was *a priori* several times lower than that of the radar (see **Fig. 3**).

[6] Also worth noting is that the radar was satisfactorily tested over a channel covered by an acrylic sheet (case "L.11"): if the signal emitted by a radar can pass through a solid material, its frequency will indeed remain the same (contrary to its speed) and the instrument will therefore be able to properly determine the velocity of a water surface.

When tested in the laboratory and looking downstream, the radar was found (**Fig. 7b**) to estimate water velocity with an uncertainty still $[p = 0.95]$ consistent with what was expected at the beginning. Nonetheless, the radar tended to estimate a lower velocity when looking downstream instead of upstream. It was also working less well over steep channels. On the one hand, it was often taking more time before displaying a velocity data. And on the other hand, it was more sensitive to its relative incidence angle: unrealistic (too low) velocity data were determined when θ was not large enough (see Section 4.2); this could explain why a velocity data taken with a rather low incidence angle (θ ≈ 53°) over a very steep channel (case "L.13b") is significantly low (see the oval in **Fig. 7b**).

It could be argued that the laboratory results underestimate the usual performances of the radar, because it has been tested very close to the water surface (Section 3.2). However, when tested in the field, the radar data (**Figs. 7-8**) were found to be consistent with those obtained in the laboratory. In particular, for four cases (**Fig. 8c-f**) it was observed that the radar clearly estimated a lower velocity when looking downstream instead of upstream.

Summarizing, even though the handheld radar has provided velocity data in the range of what was expected *a priori*, three biases (to be discussed further below) were found during this study: (1) *the tested radar does not work well at too low incidence angles,* (2) *the radar underestimates the reference data* and (3) *the radar estimates a lower velocity when looking downstream instead of upstream.*
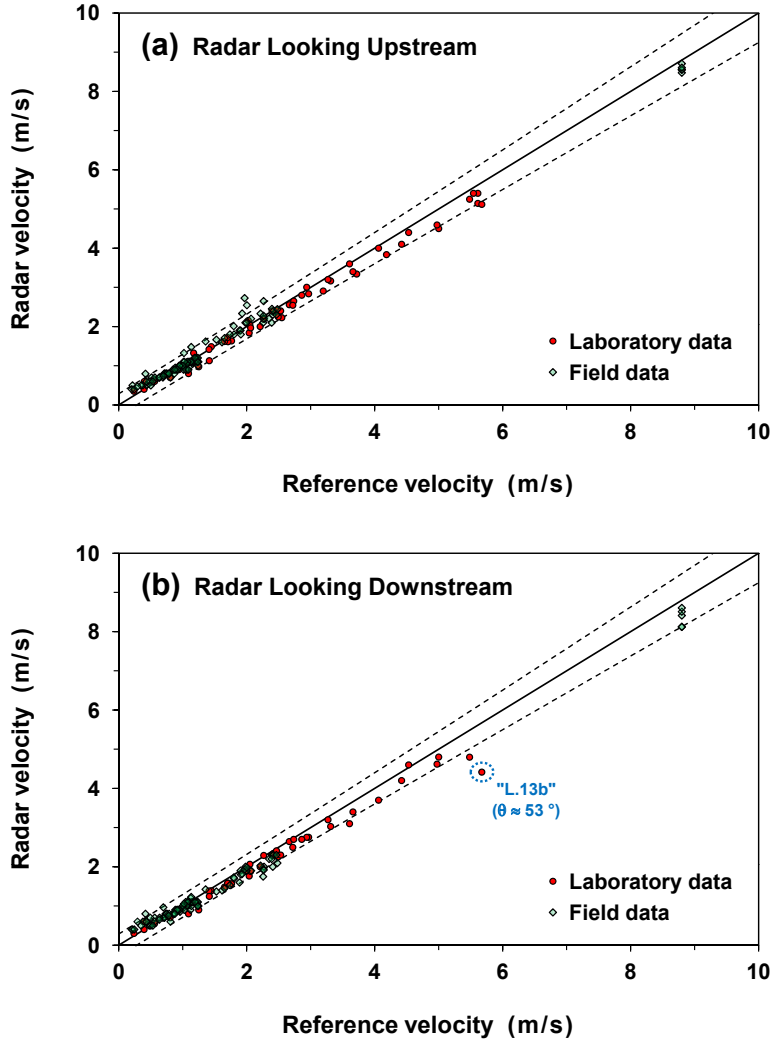
Fig. 7. Laboratory and field testing of the handheld radar:
radar vs. reference techniques (see Section 3.5).

The results are shown for all the channels listed in **Table 1**.
The dashed lines show the expected uncertainty of the radar $[p = 0.95]$.

— **3 1** —

Fig. 8. Field testing of the handheld radar: horizontal velocity profiles obtained at the water surface with the radar and with others techniques chosen as a reference.

The results are shown for all the field channels listed in **Table 1**.
The vertical line on each plot shows the maximum expected radar uncertainty $[p = 0.95]$.
The triangles at the bottom of each plot show the channel edges.

4.2. Effect of the radar's incidence angle

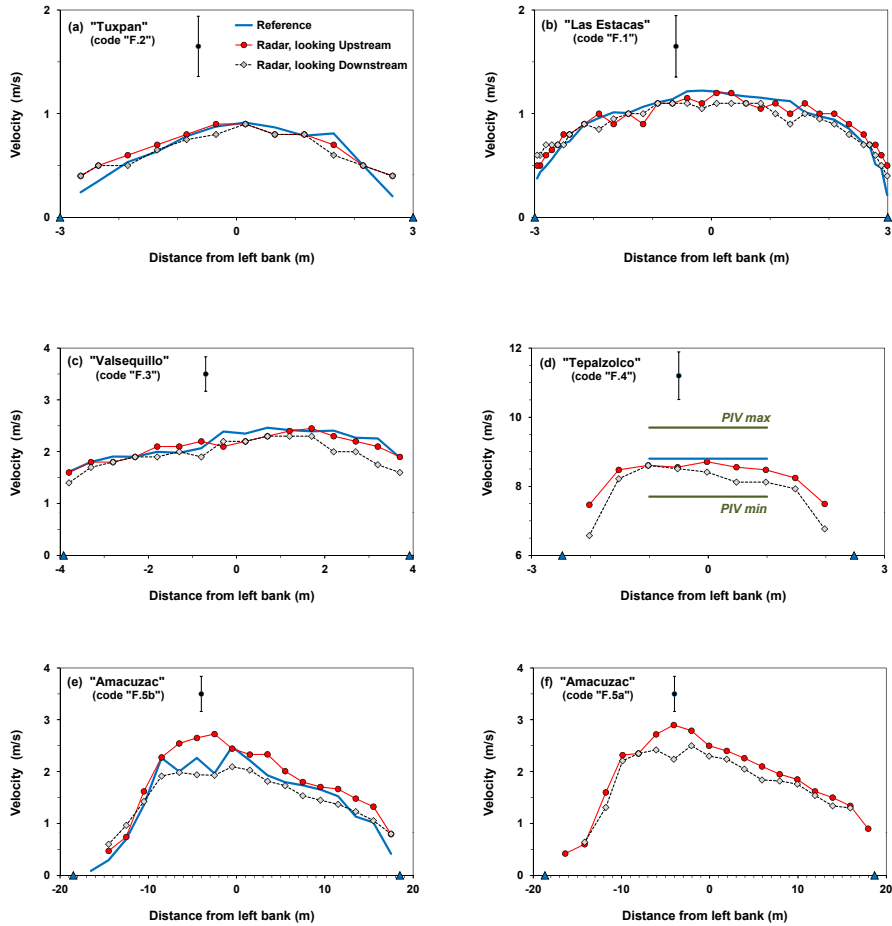Some preliminary tests were performed in the laboratory to see the range of relative incidence angles (θ) for which the radar provides reliable velocity data: measurements were taken with the radar oriented at different incidence angles, and the consistency of the radar data was evaluated. In all cases, the slope of the water surface (β) was assumed to be the slope of the channel, which was measured using an external inclinometer ("MTi"). Whereas the radar was expected to work in the range $20 \leq \theta \leq 70°$ (Section 2.4), the obtained results (**Fig. 9**) suggest that it only provides realistic data if its relative incidence angle is large enough: $\theta \geq 40°$ for moderately inclined channels (slope $\beta \leq 10°$) and $\theta \geq 50°$ for steep channels ($\beta > 10°$).
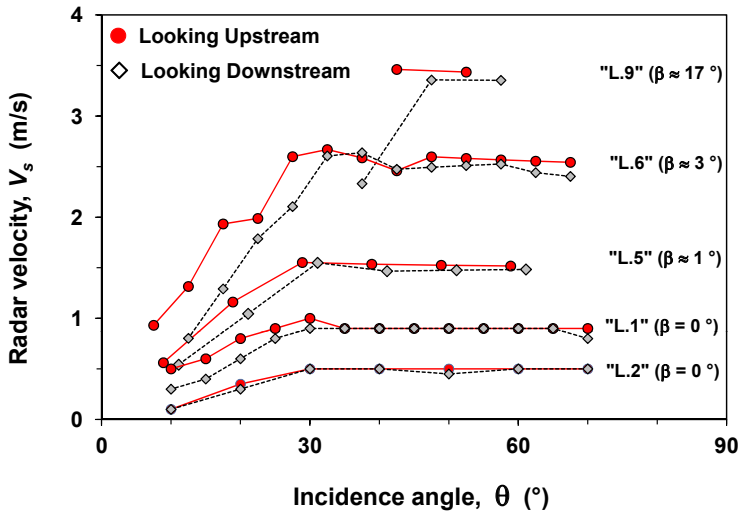
Fig. 9. Laboratory testing of the handheld radar: effect of the local incidence angle (θ) on the water velocity (V_s) estimated by the radar, when it is looking upstream (circles) or downstream (diamonds). The results are shown for five laboratory channels (codes refer to the list in **Table 1**) with different slopes (β).

The radar was found to increasingly underestimate water velocity as its relative incidence angle decreases from $\theta \approx 35°$ in horizontal channels and $\theta \approx 45°$ in steep channels (**Fig. 9**). This trend was not expected, but rather, it was thought that the radar would still work satisfactorily for a relative incidence angle as low as $\theta \approx 20°$.

- *A bias of the radar's inclinometer ?* - The trend cannot be explained by the bias of the radar's inclinometer (**Fig. 5**): in a preliminary attempt to correct for this bias, no significant improvement of the radar's performances was obtained.

- *An effect of the radar's beam width ?* - The trend could be due to the rather large beam width (12°) of the studied radar [Anonymous 2013, personal communication]. An inclined radar with a non-zero beam width should be indeed more sensitive at incidence angles lower than the nominal one (θ). In this case, the water velocity (V_s) should be estimated from the measured radial velocity (V_r) using an incidence angle smaller than the nominal one. Otherwise, the water velocity will be underestimated (see **Eq. 2**). However, this effect is pronounced only for radars with a large beam width (as the tested one) and for small incidence angles (*i.e.* as $\sin\theta \rightarrow 0$).

   In this context, it was empirically found that the experimental results shown on **Fig. 9** can be roughly explained (**Fig. 10**) by assuming that the *effective* radar's incidence angle (θ^e) is lower by 4° than the nominal incidence angle (θ). [7]

Based on the results of the preliminary testing, the radar was further tested with a relative incidence angle (θ) between 45 to 50° for moderately inclined channels ($\beta \approx 10°$) and between 50 to 60° for steep channels.

---

[7]   Due to the lack of knowledge, it was not possible to analyze more in details the effect of the radar's beam width (as a radar's expert could, although it is worth noting that the radar has not been operated according to the *far field condition during* laboratory testing; for more details, see Section A.4).

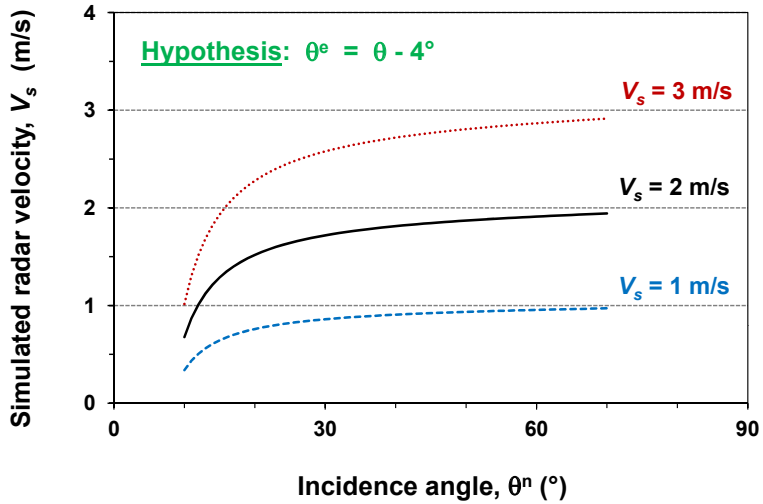**Fig. 10.** A simple simulation of the water velocity (V_s) estimated by the radar, based on the assumption that its *effective* incidence angle (θ^e) is lower by 4° than the nominal incidence angle (θ). Three cases of surface velocity (1, 2 and 3 m/s) are shown.

4.3. UNDERESTIMATION OF THE REFERENCE VELOCITIES

According to a regression analysis, the radar data were significantly different from the reference data: on the average, the radar data were lower by ≈ 5 % of the value when the radar was looking upstream (**Fig. 11a**), and lower by ≈ 8 % of the value when the radar was looking downstream (**Fig. 11b**). This trend was not expected:

- *A bad choice of the reference techniques ?* - It could be argued that the current meters used as a reference for testing the radar (Section 3.3) may have underestimated the velocity at the surface of narrow (*i.e.* aspect ratio < 5) and rectangular channels, due to the dip phenomenon. However, the radar was also tested at the central part of trapezoidal channels and of wide rectangular channels, where the dip phenomenon should not occur [Tominaga *et al.* 1989].

- *An effect of the Stokes drift ?* - There could be a difference between the radar and the reference data due to the Stokes drift, because it is accounted for by a Doppler radar, but not by the conventional current meters (*i.e.* MCC, EMV, ADV and Pitot tube). Nevertheless, the Stokes drift should be in the direction where the larger water waves propagate. Considering that the wind was small (see Section 2.5), these waves should have been mostly driven by the underlying current. In this case, the Stokes drift should have been in the direction of the current: it cannot therefore explain why the radar data were lower than the reference data.

- *A bias of the radar's inclinometer ?* - Contrary to what has been reported for the other commercial model of handheld radar [Dramais *et al.* 2013], the trend cannot be explained by the bias of the radar's inclinometer (**Fig. 5**): in a preliminary attempt to correct for this bias, no significant improvement of the radar's performances was obtained.

- *An effect of the radar's beam width ?* - Although we are not able to analyze in details the effect of the radar's beam, the underestimation of the reference velocities is rather well explained (**Fig. 11c-d**) by the simple hypothesis (Section 4.2) of an overestimation (by 4°) of the radar's *effective* incidence angle (θ^e).
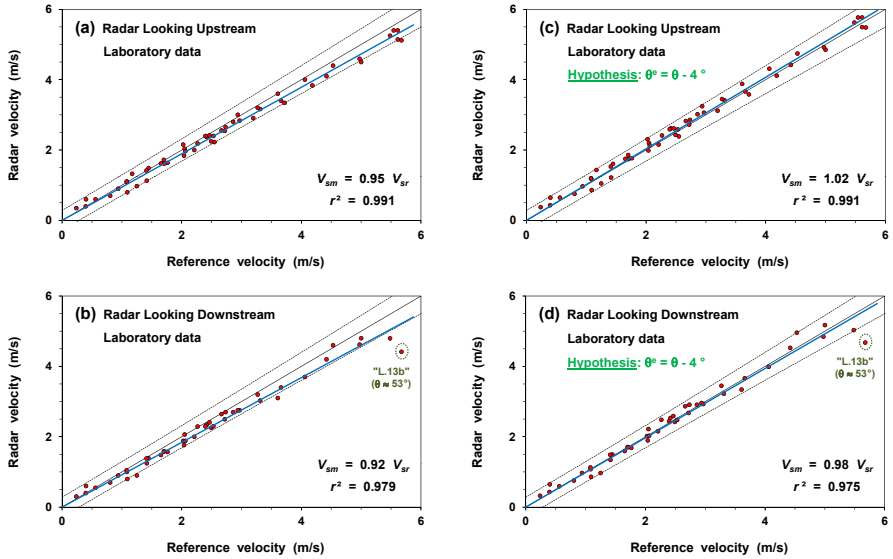
Fig. 11. Laboratory testing of the handheld radar: radar vs. conventional current meters located at ≈ 2 cm below the water surface (see Section 3.5).

The results are shown for all the laboratory channels listed in **Table 1**.
The dashed lines show the expected uncertainty of the radar $[p = 0.95]$.

The results shown on the plots of the right column are based on the assumption that the radar's *effective* incidence angle (θ^e) is lower by 4° than the nominal incidence angle (θ).

4.4. Radar looking downstream vs. looking upstream

The radar was found to usually estimate a lower velocity when looking downstream (V_s^{down}) instead of upstream (V_s^{up}). Roughly, the velocity difference ($\Delta V_s = V_s^{up} - V_s^{down}$) was increasing as a function of water velocity, when it was larger than ≈ 1 m/s (**Fig. 12**). No clear trend was found in ΔV_s as a function of other quantitative (Froude number, aspect ratio, channel slope) or qualitative (laboratory or field testing) variables listed in **Table 1** (results not shown).

It is still difficult to know why the radar was tending to estimate a lower velocity when looking downstream instead of upstream: [8]

- *A wind effect (and an inaccurate data processing) ?* - The histogram of the raw data recorded by a microwave Doppler radar (converted into surface velocities) is often skewed. Many studies performed in water tanks [*e.g.* Gade *et al.* 1998, Plant *et al.* 2004] and on the sea [*e.g.* Plant & Keller 1990] have shown that this can be due to the wind (even a light air, with a speed as low as ≈ 0.3 m/s), which produces an asymmetry in the roughness at the water surface (unless the wind is blowing perpendicularly to the radar's line-of-sight): (1) if a radar is looking *upwind*, it should record a histogram with a larger peak corresponding to the advancing ripples ($V_s + c_B$); (2) on the opposite, if the radar is looking *downwind*, it should record a histogram with a larger peak corresponding to the receding ripples ($V_s - c_B$) and (3) under those circumstances, if the radar does not process carefully the raw data (*i.e.* if it does not extract the midway point between the two theoretical peaks of the histogram, but computes an average value, or -even worse- takes the mode), the absolute value of ΔV_s could be as large as ≈ 2 × c_B, which is ≈ 0.6 m/s for the studied radar (Section 2.4).

  Since most of the observed values of ΔV_s were within ± 0.6 m/s (**Fig. 12**), they could be due to a wind effect and to an inaccurate data processing.

---

8   The hypothesis that the radar's effective incidence angle is overestimated (Sections 4.2-3) cannot explain the trend, because it is not related to the fact that the radar is looking upstream or downstream.
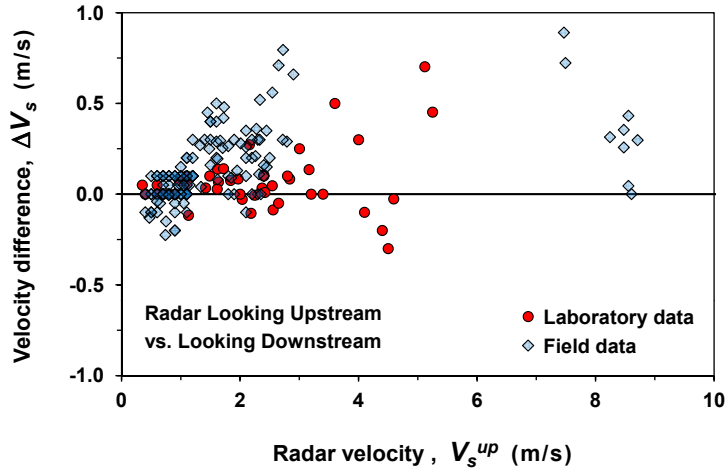
Fig. 12. Difference in velocity between the radar looking upstream and downstream (ΔV_s) as a function of the velocity measured by the radar looking upstream (V_s^{up}).

- *A hydrodynamic effect ?* - Unfortunately, the wind direction and speed have not been systematically measured during this study. However, if the observed values of ΔV_s were due to the wind, the fact that they were usually positive would mean that the wind was blowing most of the time from upstream in the studied channels. A few field observations suggest that this was not always true: above all, the observed values of ΔV_s were usually positive at the "Las Estacas" channel (**Fig. 8b**) although a light breeze was coming from downstream. In addition, larger values of ΔV_s were obtained twice at the same specific part of the "Amacuzac" river (**Fig. 8d-f**), although a light air with changing direction was blowing during testing (for more details, see Section D.1).

So, it can be argued that some of the observed values of ΔV_s were not due to a wind effect but to a hydrodynamic effect. However, still little is known about how a microwave Doppler radar responds to a rough water surface produced by the turbulence (for more details, see Section A.3):

❖ *A hydrodynamic effect and an inaccurate data processing ?* - The observed values of ΔV_s could be due to an asymmetry in the roughness at the water surface produced by the underlying current (instead of the wind) and to an inaccurate data processing by the radar: (1) the radar looking *upstream* would record a histogram of raw data with a larger peak corresponding to the advancing ripples; (2) the radar looking *downstream* would record a histogram with a larger peak corresponding to the receding ripples and (3) the radar would not be able to properly extract the midway point between the two theoretical peaks of the histogram.

❖ *A hydrodynamic effect only ?* - Finally, if the tested radar properly processes the raw data, the question arises if the observed values of ΔV_s are a general feature of microwave Doppler radars when used in open channels under clear weather conditions. For instance, a hypothesis based on the distortion of the larger water waves is proposed in Section D.2 to qualitatively explain the positive values of ΔV_s. More studies are necessary to verify this hypothesis.

5 . C O N C L U S I O N

Over the last fifteen years, a growing number of studies have shown that Doppler radar technology is a promising tool to estimate water velocity at the surface of open channels. In this context, a commercial handheld radar was tested. The testing covered a broad range of velocities (from 0.3 to at least 6 m/s) and channel types (including inclined channels). The radar was able to estimate the water velocity within $[p = 0.95] \pm 0.3$ m/s at medium velocities (from 0.3 to 3 m/s) and $\pm$ 10 % of the measured value at large velocities. Although this is not very accurate, the ease of using handheld radars still makes them attractive to quickly estimate discharge at some gauging stations and to investigate how water flows under difficult access conditions.

Even though the tested handheld radar has provided velocity data in the range of what was expected *a priori*, some biases were found during this study. On the one hand, the fact that the radar does not work well at too low incidence angles and that it underestimates the reference data could be due to the rather large radar's beam width. On the other hand, the fact that the radar was usually estimating a lower velocity when looking downstream instead of upstream is still difficult to explain.

It would be useful to go on testing radars in open channels in order to see if the trends observed during this study on a single commercial instrument (with an unknown data processing algorithm) are reproducible or not. If they are, more investigations conducted by experts would be necessary to improve the estimation of water velocity at the surface of open channels by microwave Doppler radars: currently, little is known about how these instruments respond to a rough water surface, when the roughness is due to the underlying current.

```
┌─────────────────────────────────────────────────┐
│          - A P P E N D I X    A -                │
│        S O M E    D E T A I L S                  │
│        A B O U T    R A D A R                    │
└─────────────────────────────────────────────────┘
```

A.1. DOPPLER RADARS TO STUDY WATER BODIES

Doppler radars have been used in Oceanography for fifty years, to estimate either the wind above the ocean either the superficial currents [*e.g.* Hasselmann *et al.* 1985, Lipa & Barrick 1986, Chapron *et al.* 2005]. In the last fifteen years, a growing number of studies have shown that Doppler radars can also determine the surface velocity of rivers [*e.g.* Plant *et al.* 2005, Costa *et al.* 2006]; different types of instruments have been developed for this purpose and some are now commercially available (*e.g.* "RiverSonde" from Codar Ocean Sensors, "Flo-Dar" from Marsh-McBirney, "RQ-30" from Sommer GmbH). Two broad categories of radar must be distinguished according to their signal frequency:

- *HF radar* - On the one hand, the *HF radar* [*e.g.* Lipa & Barrick 1986] sends a signal in the HF/VHF/UHF range ($f_0 \approx 3$ to 3000 MHz), which corresponds to a wavelength λ_0 between ≈ 0.1 and 100 m ($\lambda_0 = c_a / f_0$, with $c_a \approx 3 \times 10^8$ m/s); this signal is scattered by rather large (gravity) water waves.

- *Microwave radar* - On the other hand, the *microwave radar* [*e.g.* Plant & Keller 1990] sends a signal in the SHF/EHF range ($f_0 \approx 3$ to 300 GHz), which corresponds to a wavelength λ_0 between ≈ 0.001 and 0.1 m; this signal is scattered by small (capillary-gravity) water waves.

A.2. Bragg resonant condition

The theory of how a radar signal is backscattered by a water surface is not straightforward [*e.g.* Hasselmann *et al.* 1985, Plant & Keller 1990, Elfouhaily & Guérin 2004, Plant *et al.* 2004]. On the one hand, it is considered that the radar signal barely penetrates the water (not more than a few cm for a microwave signal) [*e.g.* Ulaby *et al.* 1986, Plant *et al.* 2005]. On the other hand, and for a moderately inclined radar ($20 \leq \theta \leq 70°$), the theory considers that most of the signal backscattering will be produced by periodic water waves traveling in front of the radar (either toward the radar, either away from it) and with a specific wavelength (Λ_B, m), which depends on two radar characteristics: the wavelength of the radar signal (λ_0, m) and the incidence angle (θ,°). The relation is known as the *Bragg resonant condition* (**Fig. A.1**):

$$\Lambda_B \quad = \quad \frac{\lambda_0}{2 \; \sin \theta} \tag{A.1}$$

Of course, the real shape of an agitated water surface is quite irregular. In this case, it is considered that it can be decomposed in a superposition of periodic waves, each one having a specific wave length. For instance, the frequency of the signal emitted by the studied handheld radar is $f_0 = 34.7$ GHz [Stalker Radar 2008], which corresponds to a wavelength of $\lambda_0 = 9$ mm. If such a radar is oriented with an incidence angle $\theta \approx 45°$, the water waves expected to backscatter its signal should have a wavelength $\Lambda_B \approx 6$ mm. In Hydraulics, these small waves ($\Lambda_B < 17$ mm; see Section B.1) are called *ripples* (or *capillary waves*).

A consequence of the above theory is that the raw data obtained by a Doppler radar (a time-series of Doppler shifts) above a water surface are "noisy": the water waves that backscatter the radar signal do not travel exactly at the mean velocity of the surface (V_s), because they also tend to move forward and backward at their own *phase speed* (c_B; see Section B.1). So, the histogram of the raw data recorded by a radar looking at a moving water surface (converted into surface velocities, according to **Eqs. 1-2**) should ideally show two marked peaks (not necessarily of the same amplitude): one for the advancing water waves ($V_s + c_B$) and the other for the receding ones ($V_s - c_B$). In this case, the basic operation of a Doppler radar consists in [*e.g.* Lipa & Barrick 1986, Plant *et al.* 2005]: (1) recording velocity data for a sufficiently long integration time, (2) identifying the two largest peaks in the histogram of the velocity data and (3) estimating the average velocity (V_s) as the midway point between these two peaks.
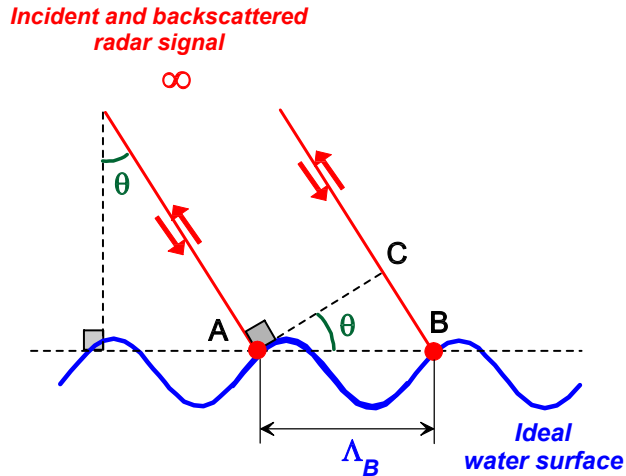

Fig. A.1. Diagram of the Bragg resonant condition in case of a monostatic radar.

The resonance occurs if the distance BC ($= \Lambda_B \times \sin\theta$)

is half the wavelength of the radar signal (λ_0).

A.3. Composite surface theory (for microwave radar)

Compared to a HF radar, the histogram of the raw data recorded by a microwave radar unfortunately does not always show two marked peaks. This is mostly explained by the *composite surface theory* [*e.g.* Hasselmann *et al.* 1985], which basically considers that the small water waves (ripples) that backscatter microwaves (Section A.2) are advected by larger waves:

- *The two peaks of the histogram can be mingled into a single one due to advection by larger waves* - Advection of ripples by larger water waves produces a broadening in the histogram of the raw radar data for two reasons: (1) the larger water waves travel at a variety of speeds (depending on their own phase speed) and (2) they tilt the ripples (producing variations in the local incidence angle of the radar). In cases where this broadening is not too severe, two peaks can still be detected in the histogram of the raw radar data. However, severe broadening causes the two peaks to be mingled into a single broad one [*e.g.* Contreras & Plant 2004, Plant *et al.* 2005].

- *One of the two peaks of the histogram can be sometimes difficult to discern* - Under certain circumstances, it may be difficult to discern one of the two theoretical peaks in the histogram of the raw radar data. Above all, many studies performed in water tanks [*e.g.* Gade *et al.* 1998, Plant *et al.* 2004] and on the sea [*e.g.* Plant & Keller 1990] have shown that this can be due to the wind (even a light air, with a speed as low as ≈ 0.3 m/s), which produces an asymmetry in the roughness at the water surface (unless the wind is blowing perpendicularly to the radar's line-of-sight): (1) if a radar is looking upwind, it should record a histogram with a larger peak corresponding to the advancing ripples $(V_s + c_B)$; (2) on the opposite, if the radar is looking downwind, it should record a histogram with a larger peak corresponding to the receding ripples $(V_s - c_B)$.

For the above reasons, complex algorithms can be necessary to properly estimate an average velocity (V_s) from the histogram of raw data recorded by a microwave radar: if data are not processed carefully (*i.e.* if the midway point between the two theoretical peaks of the histogram is not extracted), the estimated surface velocity (V_s) can be erroneous up to $\pm c_B$, where c_B is the phase speed of the water waves (ripples) that backscatter the radar signal [Plant *et al.* 2005].

It is worth noting that the composite surface theory has been extensively verified when the roughness at a water surface is due to the wind, but not so much when it is due to water turbulence:

- *Roughness due to the wind* - The effect of a roughness caused by the wind has been investigated in the sea [*e.g.* Plant & Keller 1990] and in water tanks exposed to a blower [*e.g.* Plant *et al.* 2004]. As said, the wind can produce a skewed histogram of the raw radar data. [9]

- *Roughness due to the distortion of larger water waves* - The effect of a roughness due to the distortion of larger water waves (*i.e.* the production of the so-called *bound waves*) has been also investigated in the sea [*e.g.* Plant 2003] and in water tanks exposed to a mechanical agitation [*e.g.* Gade *et al.* 1998] or to a blower [*e.g.* Plant *et al.* 2004]. In this case, the effect of the distortion of larger waves on the response of microwave radars was found to be quite similar to the effect of the wind [Plant *et al.* 2005].

- *Roughness due to the rain* - Rain drops falling on a water surface typically produces ring waves. In this case, the two theoretical peaks in the histogram of the raw radar data can be easily identified [*e.g.* Contreras & Plant 2004, Plant *et al.* 2005].

- *Roughness due to the turbulence* - The effect of a roughness due to the water turbulence still has not been investigated extensively. Although some studies have been performed in rivers in the last fifteen years, the experts [Plant *et al.* 2005] consider that "*when the short waves are produced by turbulence, the azimuth angle dependence of their intensity has not been well established to date*". In this context, it is worth noting that we could not find in the literature a study about Doppler radar performed in laboratory channels with flowing water.

---

9   An extreme situation is when the wind is blowing nearly in front or behind the radar (under no rain conditions): in this case, the smaller peak in the histogram of the raw radar's data can be so small (in fact, it can disappear into the noise baseline), that it becomes very difficult to properly process the radar data, unless the wind direction is known [Plant *et al.* 2005].

A.4. Far field condition

From a theoretical point of view, the data obtained with a radar are more difficult to interpret if the distance between its antenna and a target (L) is too small [Ulaby *et al.* 1981]. For this reason, radars are usually operated according to the *far field condition*, *i.e.* so that the distance L is larger than a minimum value (L_F); for a circular antenna (as the one of the studied radar), it is:

$$L_F \quad = \quad \frac{2\ D^2}{\lambda_0} \qquad\qquad (A.2)$$

where D is the antenna diameter (m) and λ_0 is the wavelength of the radar signal (m). For the studied radar, $\lambda_0 = 9$ mm ($f_0 = 34.7$ GHz) and $D \approx 50$ mm (diameter of the front part), which gives: $L_F \approx 0.6$ m. So, it must be recognized that the radar has not been operated according to the far field condition during laboratory testing (Section 3.2); rather, it has been located at a distance to the water surface between 0.1 and 0.3 m, which corresponds to the so-called *Fresnel zone* [Ulaby *et al.* 1981].

A.5. Footprint of the studied radar

Under the far field condition (Section A.4), the area "seen" by a radar (*footprint*) can be estimated with simple geometrical calculations (**Fig. A.2**). Assuming that the signal is sent as a cone, this area should be an ellipse with the following longitudinal (D_L) and transversal (D_T) diameters:

$$D_L = L \, \cos(\theta) \left[\tan\left(\theta + \frac{\gamma}{2} \right) - \tan\left(\theta - \frac{\gamma}{2} \right) \right] \qquad \text{(A.3a)}$$

$$D_T = 2 \, L \, \tan\left(\frac{\gamma}{2} \right) \qquad \text{(A.3b)}$$

where L (m) is the distance between the radar and the water surface in the line-of-sight direction, θ (°) is the local incidence angle and γ (°) is the aperture of the cone containing most of the radar signal (*3 dB beam width*). Considering $\gamma = 12°$ [Stalker Radar 2008] and $\theta \approx 45°$ (the typical incidence angle of the radar used during this study), it gives $D_T \approx 0.2 \times L$ and $D_L \approx 0.3 \times L$.
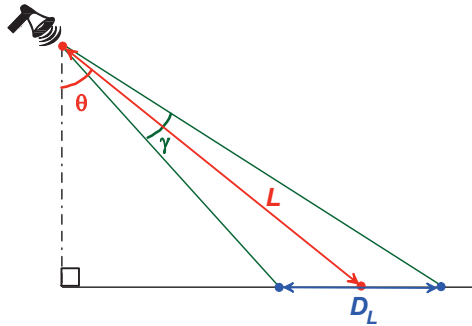

Fig. A.2. Diagram of the radar footprint, in the plane of incidence (assuming that the radar is operated according to the far field condition).

<div style="border:1px solid black; padding:10px;">

- A P P E N D I X   B -

S O M E   D E T A I L S

A B O U T   W A T E R   W A V E S

</div>

B.1. PHASE SPEED

The *phase speed* of a water wave is the velocity at which its shape (crests and troughs) moves along the water surface. For a deep open channel (water depth h large enough, so that: $k \times h >> 1$), the phase speed of a (gravity - capillary) water wave is [*e.g.* Ulaby *et al.* 1986]:

$$ c \quad = \quad \sqrt{ \frac{g}{k} \; + \; \frac{\sigma_w \, k}{\rho_w} } \tag{B.1} $$

where $k = 2 \times \pi \,/\, \Lambda$ is the angular wavenumber (m^{-1}), Λ is the water wavelength (m), σ_w is the water's surface tension ($\approx 73 \times 10^{-3}$ N/m), ρ_w is the water density (≈ 1000 kg/m^3) and g is the acceleration of gravity (≈ 9.8 m/s^2). [10] For instance, the water waves expected to backscatter the signal of the studied radar should have a wavelength $\Lambda_B \approx 6$ mm (Section A.2); in this case, their phase speed should be $c_B \approx 0.3$ m/s.

---

10   According to **Eq. B.1**, the phase speed of water waves must have a minimum value ($c_{min} \approx 0.23$ m/s) at one particular wavelength, which is: $L_{min} \approx 17$ mm. The properties of water waves with a wavelength larger than L_{min} are mostly controlled by the acceleration of gravity (i.e., the first term of **Eq. B.1**): this is the gravity wave regime. On the opposite, the properties of water waves with a wavelength smaller than L_{min} are mostly controlled by the surface tension (i.e., the second term of **Eq. B.1**): this is the capillary wave regime.

B.2. STOKES DRIFT

The *Stokes drift* is a displacement of a water surface produced by the water waves themselves. Due to this phenomenon, a water surface moves faster than what advects it (the combined effect of the wind and the underlying current). This is because: (1) water particles rotate into the waves (*orbital motion*) in the direction of what advects the surface and (2) the speed of particles at the crests of a water wave is forward and slightly larger than the speed at the troughs, which is backward. For gravity water waves ($\Lambda \gg 17$ mm), the Stokes drift at the water surface is [*e.g.* Monismith & Fong 2004]:

$$U_s \quad = \quad (a\,k)^2 \ c_{GW} \quad \frac{\cosh(2\,k\,h)}{2\ \sinh^2(k\,h)} \tag{B.2a}$$

$$c_{GW} \quad = \quad \sqrt{\frac{g\ \tanh(k\,h)}{k}} \tag{B.2b}$$

where $k = 2 \times \pi / \Lambda$ is the wavenumber (m^{-1}), Λ is the wavelength (m), a is the wave amplitude (m), h is the water depth (m) and g is the acceleration of gravity (≈ 9.8 m/s^2). Two situations must be distinguished for the studied channels (**Table 1**):

- *Laboratory channels* - Considering: $h \geq 0.03$ m, $\Lambda \leq 0.2$ m and the fact that there was no breaking waves (that is: $a \leq 0.072 \times \Lambda$ [*e.g.* Gemmrich 2005]), a rather small Stokes drift was expected in the laboratory: $U_s \leq 0.14$ m/s.

- *Field channels* - Considering: $h \geq 0.25$ m and $\Lambda \leq 1$ m, the Stokes drift may have been sometimes large in the field: $U_s \leq 0.27$ m/s, even in the case of non-breaking waves.

B.3. Froude number

Considering a channel with shallow water waves and a trapezoidal cross section, the *Froude number* (*Fr*) was computed as:

$$Fr \approx \frac{V_m}{\sqrt{g\left(\frac{B+b}{2B}\right)h}} \tag{B.3}$$

where V_m is the mean water velocity in the channel (m/s), h is the water depth (m), b is the channel width at the bottom (m), B is the channel width at the surface (m) and g is the acceleration of gravity (≈ 9.8 m/s^2).

The mean velocity was estimated as: $V_m = \kappa \times V_s$, where V_s is the surface velocity (m/s) measured at the center of a channel and κ is a coefficient (-). Considering that most of the studied channels were wide (*aspect ratio* $\nu > 5$), we took $\kappa \approx 0.85^2 \approx 0.72$ [*e.g.* ISO 2007, Le Coz *et al.* 2010].

C.1. Pitot tube

The Pitot tube is a current meter often taken for granted today [Brown 2003]. Although often used in Aerodynamics (*e.g.* to determine the speed of an airplane), it is not anymore commonly used in Hydraulics. However, the Pitot tube is still attractive to measure large water velocities, at least in the laboratory.

A commercial Pitot tube (model 630, Lambrecht, Germany) connected to two water manometers was used to determine the velocity in laboratory channels (**Fig. C.1**). In this case, the water velocity was computed as:

$$V \quad = \quad \sqrt{2\,g\,\Delta h} \tag{C.1}$$

where Δh is the measured difference in level between the two manometers (m) and g is the acceleration of gravity ($= 9.78$ m/s^2 in Cuernavaca, Mexico). The theoretical uncertainty of the Pitot tube is deduced from the previous equation [JCGM 2008]:

$$U(V) \quad = \quad \sqrt{\frac{g}{2\,\Delta h}} \; \times \; U(\Delta h) \tag{C.2}$$

where $U(\Delta h)$ is the uncertainty of the measured difference in level; during this study, an uncertainty [$p = 0.95$] of $\pm\, 0.01$ m was easily achieved.

Fig. C.1. Pitot tube: (a) instrument, (b) water manometers and (c) laboratory testing.

C.2. PARTICLE IMAGE VELOCIMETRY

To estimate the surface velocity at the "Tepalzolco" rapid (**Fig. C.2**), a simple PIV technique was used: (1) some marks were left on the channel edges (spacing = 1 m), (2) a video camera placed in the center of the channel was used to film the water surface (upstream and then downstream, speed of recording = 30 frames/s), (3) assuming that the camera's objective was not producing too much distortion, the recorded images were digitally processed so that a grid was drawn over the plane corresponding to the water surface and (4) the number of image-frames necessary for a floating object (whitecap) to travel over a given distance was manually counted. A single velocity data was then estimated as:

$$V \quad = \quad \Delta L \, / \, \Delta t \tag{C.3}$$

where ΔL is the travelled distance (m) and Δt is the measured duration (s).

The theoretical uncertainty of the technique is deduced from the previous equation [JCGM 2008]:

$$U(V) \quad = \quad V \times \sqrt{\left(\frac{U(\Delta L)}{\Delta L} \right)^2 + \left(\frac{U(\Delta t)}{\Delta t} \right)^2} \qquad \text{(C.4)}$$

At the "Tepalzolco" rapid, the water velocity was $V \approx 9$ m/s and the observable distance was $\Delta L = 3$ m, which gives $\Delta t \approx 0.3$ s. Considering $U(\Delta L) = 0.05$ m and $U(\Delta t) = 0.016$ s (*i.e.* half a video frame), the uncertainty [$p = 0.95$] for a single velocity estimation was expected to be $U(V) = 0.5$ m/s. Because this is not accurate, 30 replicates were made, which should give the following uncertainty for the average: $U(V°) = U(V) / \sqrt{30} = 0.1$ m/s.

It is worth noting that a classical LSPIV algorithm [*e.g.* Le Coz *et al.* 2010] would have been difficult to use at the "Tepalzolco" rapid, because the flow field was not steady at a short time scale due to rolling waves passing every ≈ 6 seconds. In this case, the simple PIV technique was used to estimate three surface velocity data: in front, at the crest and behind the rolling waves. After that, a mean value was computed from these data (**Table C.1**).
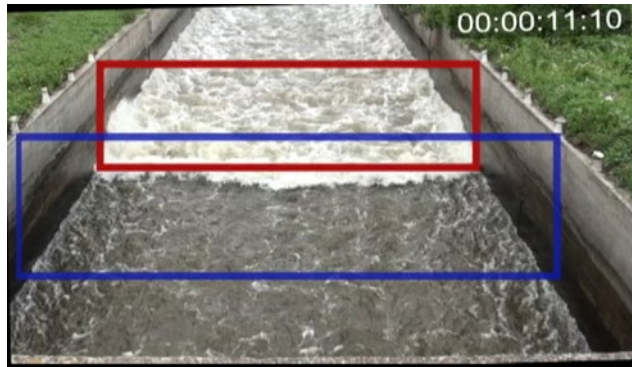

Fig. C.2. PIV at the "Tepalzolco" rapid: digitized image.

Table C.1. Surface velocities estimated by a simple PIV technique at the middle part of the "Tepalzolco" rapid (code "F.4" of **Table 1**).

Camera orientation	Estimated velocity (m/s) [a]			
	In front of the rolling waves	At the crest of rolling waves	Behind the rolling waves	Mean value
Looking Upstream	8.0 (0.3)	9.5 (0.3)	9.1 (0.3)	8.9
Looking Downstream	7.7 (0.6)	9.7 (0.6)	9.1 (0.5)	8.8

[a] The mean and the standard deviation of 30 replicates are shown.

D.1. Wind conditions during field testing

Except at the "Valsequillo" channel (case "F.3") where the wind was blowing more than usual (**Fig. D.1a**), we have unfortunately not measured the wind speed during the testing of the handheld radar. However, some qualitative observations -based on human sensations and the observation of trees- about the wind direction and intensity have been made in the field (**Table D.1**). These observations suggest that the hypothesis of a wind effect (Section 4.4) is not sufficient to explain the observed velocity differences between the radar looking upstream and downstream (ΔV_s):

- *"Valsequillo" channel (case "F.3")* - It must be recognized that the wind was coming from upstream during testing at the "Valsequillo" channel. Nonetheless, the velocity difference ΔV_s was larger *at a specific part* of the channel, *i.e.* near the right bank (**Fig. 8c**). This could be due to more turbulent flow conditions (**Fig. D.1b**), caused by a channel curvature located upstream.

- *"Tepalzolco" rapid (case "F.4")* - Although no attempt was made to determine the wind speed and direction very close to the water surface, there was virtually no wind ≈ 2 m above the surface during testing at the "Tepalzolco" rapid. In this case, the velocity difference ΔV_s (**Fig. 8d**) could be due to the passing of rolling waves (**Fig. D.1c**).

- *"Amacuzac" river (cases "F.5a" and "F.5b")* - During testing at the "Amacuzac" river, the velocity difference ΔV_s was larger *at a specific part* of the river, *i.e.* between the middle and the left bank (**Figs. 8e-f**). This could be due to more turbulent flow conditions with water waves breaking downward (**Fig. D.1d**), probably caused by a rocky bottom located upstream.

- *"Las Estacas" channel (case "F.1")* - Although the wind was coming from downstream during testing at the "Las Estacas" channel, there was no evidence of negative velocity differences ΔV_s (**Fig. 8b**), as one would expect in case of a wind effect (Section 4.4).

Table D.1. Wind conditions during the field testing of the studied radar.

Code	Site	Wind [a]		Comment about the water surface at the studied channels
		Intensity	Coming from	
F.1	*Las Estacas* (29/12/2011)	Light breeze	Downstream	Some boils at the middle part of the channel
F.2	*Tuxpan* (07/06/2011)	Calm	*n.a.*	Low agitated water surface
F.3	*Valsequillo* (20/06/2012)	Gentle breeze	Upstream	More turbulence (and foam) near the right bank
F.4	*Tepalzolco* (21/06/2012)	Calm	*n.a.*	Rapid with rolling waves
F.5a	*Amacuzac* (15/08/2012)	Light air	Changing direction	River with breaking waves between the middle part and the left bank
F.5b	*Amacuzac* (21/08/2012)			

[a] According to the human sensations and the observation of trees.

(a)

(b)

(c)

(d)

Fig. D.1. Water surface at some channels where the radar was tested:
(a) "Valsequillo" channel (code "F.3") where the maximum wind intensity (a gentle breeze) was observed, (b) "Valsequillo" channel (code "F.3") seen from upstream and with more turbulence (and foam) near the right bank, (c) "Tepalzolco" rapid (code "F.4") seen from downstream and with rolling waves and (d) "Amacuzac" river (code "F.5") seen from downstream and with breaking waves near the left bank.

D.2. A hypothesis about microwave radars under clear weather

The fact that the tested radar does not provide the same average velocity data when looking downstream or upstream (Section 4.4) could be due to a *combination* of two phenomena:

- *Orbital motion into water waves* - Due to the orbital motion into waves, a water surface does not move only horizontally, but also vertically. A Doppler radar should be sensitive to this vertical movement [*e.g.* Romeiser & Thompson 2000, Plant *et al.* 2004, Chapron *et al.* 2005]. Nevertheless, if the water waves that backscatter its signal (*i.e.* ripples for a microwave radar) cover the entire water surface, this phenomenon should only broaden the histogram of velocities recorded by the radar, but not affect the average velocity computed from this histogram (unless the averaging time is short; [*e.g.* Romeiser & Thompson 2000]).

- *Uneven spatial distribution of ripples* - Under clear weather conditions (no rain drops or wind blowing), the ripples that backscatter microwaves (at least those emitted by a *Ka-band* radar, as the tested one) are however probably not evenly distributed over the water surface. Many of these are indeed produced by the distortion of steep larger waves, and in this case, several theoretical [*e.g.* Hung & Tsai 2009] and laboratory [*e.g.* Gade *et al.* 1998, Plant *et al.* 2004] studies have shown that their distribution depends on the wavelength of the carrier waves (Λ_C): although ripples tend to be located over the whole surface of small carrier waves ($\Lambda_C \leq 0.05$ m), they tend to be located only at the forward part of intermediate waves ($0.05 \leq \Lambda_C \leq 0.3$ m; due to wave distortion) [11] and at the crest of the largest ones ($\Lambda_C \geq 0.3$ m; due to micro-breaking).

---

11   In this case, the wavelength of ripples is larger near the crest of larger waves and smaller further from the crest.

So, if a microwave radar only detects ripples located on a very specific part of larger waves, the histogram of the recorded radial velocities should be shifted by a quantity that is the projection of the velocity vector at this specific part $(\vec{V}_{GW})$ over the radar line-of-sight. In this case, the average velocity computed from the histogram of radial velocities would depend on the radar incidence angle. Given this argumentation, the fact that the studied radar estimated a lower water velocity when looking downstream instead of when looking upstream could be qualitatively explained if the ripples that backscatter its signal are located at the forward and bottom part of larger water waves, because $\vec{V}_{GW}$ is oriented upward and backward in this case (**Fig. D.2**).

So, the question is open to know if the trend observed during this study is due to an imperfection in the studied radar or to a general feature of microwave Doppler radars when used in open channels under clear weather conditions. If this is a general feature, the question that follows would be to know if the trends can be corrected with an appropriate data processing algorithm (see Section A.3); unfortunately, the one used by the studied radar is a "black box" and it is not possible to retrieve the raw radar data (*i.e.* a time-series of Doppler shifts recorded during one velocity determination) in order to guess how they are processed.
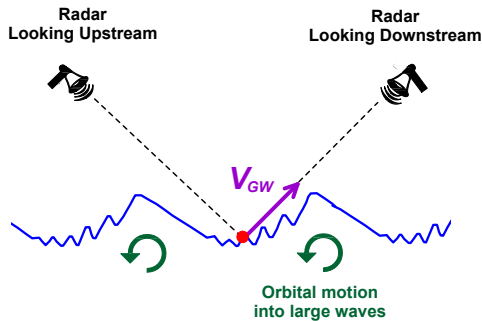

Fig. D.2. Hypothesis for qualitatively explaining why the tested radar was usually estimating a lower velocity when looking downstream instead of upstream: under clear weather conditions, the ripples that backscatter the radar signal would be located only at the forward and bottom part of larger waves, where the surface velocity vector $(\vec{V}_{GW})$ is oriented upward and backward.

<div style="border: 1px solid black; text-align: center; padding: 10px;">

R E F E R E N C E S

</div>

Brown GO. (2003). – Henry Darcy's perfection of the Pitot tube. *In*: Brown GO, Garbrecht JD & Hager WH (ed.), *Henry PG Darcy and other pioneers in hydraulics: contributions in celebration of the 200th birthday of Henry Philibert Gaspard Darcy*. ASAE, Reston (VA). pp. 14-23.

Chapron B, Collard F, Ardhuin F. (2005).– Direct measurements of ocean surface velocity from space: Interpretation and validation. *J. Geophysical Res.* **110**: paper C07008.

Contreras RF, Plant WJ. (2004).– Ku-band backscatter from the Cowltiz River: Bragg scattering with and without rain. *IEEE Trans. Geosci. Rem. Sensing* **42 (7):** 1444-1449.

Corato G, Moramarco T, Tucciarelli T. (2011).– Combining flow routing modelling and direct velocity measurement for optimal discharge estimation. *Hydrol. Earth Syst. Sci. Discuss.* **8:** 2699–2738.

Costa JE, Cheng, RT, Haeni FP, Melcher N, Spicer KR, Hayes E, Plant W, Hayes K, Teague C, Barrick D. (2006).– Use of radars to monitor stream discharge by noncontact methods. *Water Resour. Res.* **42:** paper W07422.

Decatur Electronics. (2011).– *SVR (Surface Velocity Radar) - User's Manual (Rev. 02/08/2011)*. Decatur Electronics Europe Inc., Kokkola (Finland). 45 p.

Dramais G, Le Coz J, Gallavardin A, Duby P, Hauet A, Laronne J. (2011).– Mesures sans contact des débits de crue: avancées et perspectives. *In*: Mono M. O. (ed.), *Proc. ECOTECHS' 2011 (Capteurs et Systèmes de Mesures pour les applications environnementales)*, CEMAGREF, 17-18 October 2011, Montoldre (France).

Dramais G., Le Coz J., Le Boursicaud R., Hauet A., Lagouy M. (2013).– Jaugeage para radar mobile: protocole et résultats [paper HM-044]. *In*: Biton B. (ed.), *Proc. "Hydrométrie 2013 (SHF)"*, Paris, 15-16 May 2013. [ISBN 978-2-906831-94-0]

Elfouhaily TM, Guérin CA. (2004).– A critical survey of approximate scattering wave theories from random rough surfaces. *Waves in Random and Complex Media* **14:** 1–40.

Fujita I, Watanabe H, Tsubaki R. (2007). – Development of a non-intrusive and efficient flow monitoring technique: the space-time image velocimetry (STIV). *Int. J. River Basin Management* **5 (2):** 105-114.

Fulton J, Ostrowski J. (2008). – Measuring real-time streamflow using emerging technologies: radar, hydroacoustics, and the probability concept. *J. Hydrol.* **357:** 1-10.

Gade M, Alpers W, Ermakov SA, Huehnerfuss H, Lange PA. (1998).– Wind wave tank measurements of bound and freely propagating short gravity-capillary waves. *J. Geophys. Res.* **103**: 21697-21710.

Gemmrich J (2005).– On the occurrence of wave breaking. *In*: Muller P. & Henderson D. (ed.), *Proc. 4th Aha Huliko'a Hawaian Winter Workshop on Rogue Waves*, Univ. Hawaii, School of Ocean and Earth Science and Technology, 24-28 January 2005. pp 123-130.

Hasselmann K, Raney RK, Plant WJ, Alpers W, Shuchman RA, Lyzenga RA, Rufenach CL, Tucker MJ. (1985).– Theory of SAR ocean wave imaging: a MARSEN view. *J. Geophys. Res.* **90**: 4659-4686.

Hubbard EF, Schwarz GE, Thibodeaux KG, Turcios LM. (2001).– Price current-meter standard rating development by the U.S. Geological Survey. *J. Hydraul. Eng.* **127:** 250–257.

Hung LP, Tsai WT. (2009). – The formation of parasitic capillary ripples on gravity–capillary waves and the underlying vortical structures. *J. Physical Oceanography* **39**: 263-289.

ISO. (2007).– *Hydrometry - Measurement of liquid flow in open channels using current-meters or floats (ISO 748: 2007)*. International Organization for Standardization (ISO), Genève.

JCGM. (2008).– *Evaluation of measurement data — Guide to the expression of uncertainty in measurement (JCGM 100:2008)*. Working Group 1 of the Joint Committee for Guides in Metrology (JCGM/WG1), Paris.

Jendzurski J, Paulter NJ. (2008). – Calibration of speed enforcement down-the-road radars. *J. Res. Natl. Inst. Stand. Technol.* **114:** 137-148.

Le Coz J, Hauet A, Dramais G, Pierrefeu G. (2010).– Performance of image-based velocimetry (LSPIV) applied to flash-flood discharge measurements in Mediterranean rivers. *J. Hydrol.* **394:** 42-52.

Lee JS, Julien PY. (2006).– Electromagnetic wave surface velocimetry. *J. Hydraul. Eng.* **132:** 146-153.

Lipa BJ, Barrick DF. (1986).– Extraction of sea state from HF radar sea echo. *Radio Sci.* **21**: 81-100.

Monismith SG, Fong DA. (2004).– A note on the potential transport of scalars and organisms by surface waves. *Limnology and Oceanography* **49:** 1214-1217.

Negrel J, Kosuth P, Bercher N. (2011).– Estimating river discharge from earth observation measurements of river surface hydraulic variables. *Hydrol. Earth Syst. Sci.* **15**: 2049–2058.

Newton RU, McEvoy KI. (1994).– Baseball throwing velocity: a comparison of medicine ball training and weight training. *J. Strength & Conditioning Res.* **8:** 198-203.

Plant WJ. (2003). – A new interpretation of sea-surface slope probability density functions. *J. Geophys. Res.* **108 (C9):** 3295.

Plant WJ, Keller WC. (1990).– Evidence of Bragg scattering in microwave Doppler spectra of sea return. *J. Geophys. Res.* **95 (C9):** 16299-16310.

Plant WJ, Dahl PH, Giovanangeli JP, Branger H. (2004).– Bound and free surface waves in a large wind-wave tank. *J. Geophys. Res.* **109**: Paper C10002.

Plant WJ, Keller WC, Hayes K. (2005). – Measurement of river surface currents with coherent microwave systems. *IEEE Transactions on Geoscience and Remote Sensing* **43:** 1242-1257.

Rantz SE & Col. (1982). – *Measurement and computation of streamflow: Volume 1 - Measurement of stage and discharge (USGS Water Supply Paper 2175)*. US Government Printing Office, Wahsington DC. 284 p.

Romeiser R, Thompson DR. (2000).– Numerical study on the along-track interferometric radar imaging mechanism of oceanic surface currents. *IEEE Trans. on Geosci. and Remote Sensing* **38**: 446-458.

Smith KJ, Janson SD, Smith KT. (2003).– *Radar device for measuring water surface velocity.* US Patent 2003/0058158.

Song HS, Zhang LZ, Liu W. (2006).– Comparing test and analysis on flow velocity measurement with handheld radar current meter. *[Chinese] Automation in Water Resources and Hydrology* **1:** 30-32.

Stalker Radar. (2008). – *Stalker Pro II SVR - Operator Manual (document 011-0098-00 Rev. C).* Stalker Radar / Applied Concepts Inc., Plano (TX). 23 p.

Sung-Kee Y, Dong-Su K, Kwon-Kyu Y, Meyong-Su K, Woo-Yul J, Jun-Ho L, Yong-Seok K, Ho-Jun Y. (2012).– Comparison of flood discharge and velocity measurements in a mountain stream using electromagnetic wave and surface image. *[Korean] Journal of the Environmental Sciences* **21:** 739-747.

Szupiany RN, Amsler ML, Best JL, Parsons DR. (2007).– Comparison of fixed-and moving-vessel flow measurements with an aDp in a large river. *J. Hydraul. Eng.* **133 (12):** 1299-1309.

Tominaga A, Nezu I, Ezaki K, Nakagawa H. (1989).– Three-dimensional turbulent structure in straight open channel flows. *J. Hydraul. Res.* **27 (1):** 149-173.

Turnipseed DP, Sauer VB. (2010).– *Discharge measurements at gaging stations ("U. S. Geological Survey techniques and methods", Book 3, Section A, Chapter 8).* USGS, Denver (CO).

Ulaby FT, Moore RK, Fung AK. (1981).– *Microwave remote sensing: active and passive, Vol. I - Fundamentals and radiometry.* Addison-Wesley, Advanced Book Program, Reading, Norwood (MA).

Ulaby FT, Moore RK, Fung AK. (1986).– *Microwave remote sensing: active and passive, Vol. III - From theory to applications.* Addison-Wesley, Advanced Book Program, Reading, Norwood (MA).

Zolezzi G, Zamler D, Laronne JB, Salvaro M, Piazza F, Le Coz J, Welber M, Dramais G. (2011).– A systematic test of surface velocity radar (SVR) to improve flood discharge prediction (Poster H51I-1332). *In*: *AGU Fall Meeting 2011*, AGU, San Francisco (CA), 5-9 December 2011. [only the abstract is available]